J Bone Miner Metab (2008) 26:298–300
DOI 10.1007/s00774-007-0817-1

CASE REPORT

Masayuki Tanemoto · Akira Uruno · Takaaki Abe
Sadayoshi Ito

Hypocalcemia in a patient with severe hypertension and surgically induced relative hypoparathyroidism

Received: August 7, 2007 / Accepted: September 7, 2007

Key words parathyroid autotransplantation · hypoparathyroidism · hyperphosphatemia · hypocalcemia · hypertension

of hypocalcemia. However, because the renal function was relatively preserved, the impaired parathyroid reserve was suspected to have caused hypocalcemia. The present case indicates that careful monitoring of Ca and iP is needed in the patients with impaired parathyroid reserve.

Introduction

Parathyroid hormone (PTH), vitamin D, and calcitonin play pivotal roles in the regulation of the serum concentration of calcium ion (Ca) [1]. Under the effect of these hormones, three organs mainly take part in the Ca homeostasis: (a) the intestinal tract absorbs Ca from the dietary intake; (b) the bone reserves Ca in the form of calcium phosphate; and (c) the kidney excretes Ca in the urine. Because the solubility of calcium phosphate depends on the concentration of Ca and inorganic phosphate (iP) in any solution, the serum concentration of iP affects that of Ca; hyperphosphatemia induces hypocalcemia [2].

The three main organs for the Ca homeostasis also participate in iP homeostasis, but the renal handling is the primary determinant of the serum iP concentration [2–4]. With impaired renal function, the renal excretion of iP decreases, and then hyperphosphatemia and hypocalcemia develop [2]. Intercompartmental shift of iP also markedly affects the serum iP because the intracellular compartment contains a large amount of iP [2,5,6]. However, except for a large amount of iP load, such as severe rhabdomyolysis and large-volume tumor lysis, the kidney can excrete iP loads, and hypocalcemia secondary to hyperphosphatemia is rarely seen with the preserved renal function [2,7].

Here we report a case of hypocalcemia with severe hypertension and an autotransplanted parathyroid. Hyperphosphatemia caused by the iP load from hypertensive organ damage might have contributed to the pathogenesis

M. Tanemoto (✉) · A. Uruno · T. Abe · S. Ito
Division of Nephrology, Hypertension and Endocrinology, Department of Medicine, Tohoku University Graduate School of Medicine, 1-1 Seiryo-machi, Aoba-ku, Sendai, Miyagi 980-8574, Japan
Tel. +81-22-717-7163; Fax +81-22-717-7168
e-mail: mtanemoto-tky@umin.ac.jp

Case report

Severe hypertension (>210/120 mmHg) was noted in a 39-year-old man with an episode of loss of consciousness. Without any apparent intracranial abnormalities by computed tomographic examination, hypertensive deterioration of the central nervous system was suspected, and he was referred to our department. At the age of 30, he had total thyroidectomy for a papillary carcinoma of the right thyroid gland, and a parathyroid gland was autotransplanted in the left sternomastoid. Although calcium and vitamin D supplementation was needed just after the surgery, his serum Ca and iP concentration could be maintained around 8.5 mg/dl and 3.0 mg/dl, respectively, without any supplementation subsequently. At the age of 32, with detection of high arterial blood pressure (BP, 172/110 mmHg) a diagnosis of essential hypertension was made, and antihypertensive treatment had been started. However, he discontinued the treatment because he had been asymptomatic until the episode of the loss of consciousness.

On initial physical examination, tachycardia (91 bpm) and prominent hypertension (235/121 mmHg) were detected. Examination of the ocular fundi revealed severe hypertensive change (Keith–Wagener grade 3) in both eyes. During BP measurement, Trousseau's sign appeared. Chvostek's sign and elongated QTc interval on electrocardiogram were also noted, and blood analysis revealed hypocalcemia (5.8 mg/dl) with hyperphosphatemia (5.4 mg/dl). The initial blood and urine analyses (Table 1) also revealed high serum lactate dehydrogenase (LDH, 762; normal, 119–219 IU/l) and creatinine phosphokinase (CPK, 727; normal, 50–197 IU/l). Mild renal dysfunction [serum creatinine (Cr) 1.7 mg/dl with creatinine clearance (CCr) 49 ml/min] accom-

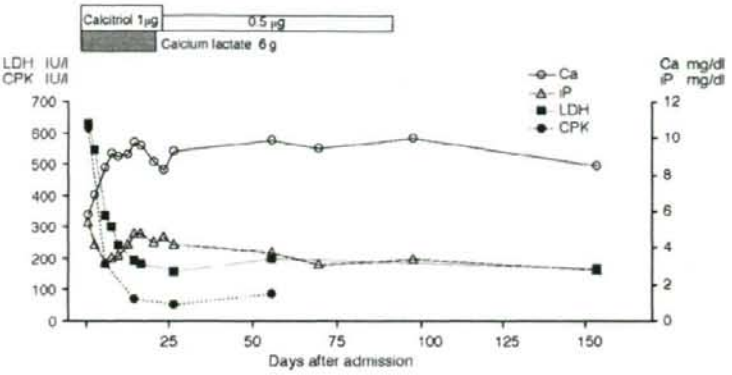

Fig. 1. Clinical course. *iP*, inorganic phosphate; *LDH*, lactate dehydrogenase; *CPK*, creatinine phosphokinase

Table 1. Laboratory data on admission

Complete blood count			
WBC	$9.2 \times 10^3/\mu l$		
RBC	$4.81 \times 10^6/\mu l$		
Hb	14.0 g/dl		
Ht	40.7%		
Plt	$208 \times 10^3/\mu l$		
Blood chemistry			
T-Bil	1.2 mg/dl	CRP	0.5 mg/dl
AST	32 IU/l	Haptoglobin	6.8 mg/dl
ALT	19 IU/l		
LDH	762 IU/l	TSH	0.156 μIU/ml
CPK	727 IU/l	Free T4	2.20 ng/dl
TP	7.2 g/dl	Free T3	2.2 pg/ml
Alb	4.0 g/dl	Intact PTH	40.8 pg/ml
BUN	23 mg/dl	1,25(OH)$_2$ vitamin D$_3$	41 pg/ml
Cr	1.7 mg/dl		
Na	141 mEq/l		
K	3.7 mEq/l		
Cl	99 mEq/l		
Ca	5.8 mg/dl		
Mg	2.1 mg/dl		
iP	5.4 mg/dl		
Urinalysis			
Protein	(3+)	Protein	1.24 g/gCr
Glucose	(−)	Na	54 mEq/gCr
OB	(1+)	K	23.4 mEq/gCr
Sediment		Cl	48 mEq/gCr
RBC	<4 /HPF	Ca	20 mg/gCr
WBC	(−)	iP	420 mg/gCr
Cast	(−)	CCr	49 ml/min

panied by proteinuria (1.24 g/gCr) was also noted. Thyroid hormone was sufficiently supplemented by administration of levothyroxine; thyroid-stimulating hormone (TSH) was 0.156 μIU/ml (normal, 0.310–4.690 μIU/ml), free T4 2.20 ng/dl (normal, 0.71–1.85 ng/dl), and free T3 2.2 pg/ml (normal, 2.5–4.3 pg/ml).

Treatment with antihypertensives was immediately started against severe hypertension. With administration of long-acting nifedipine (40 mg/day), BP decreased gradually. Additional administration of temocapril (starting from 0.5 mg/day to final dose of 4 mg/day), trichlormethiazide (1 mg/day), and olmesartan (starting from 10 mg/day to final dose of 40 mg/day) normalized his BP. With reduction of BP, the amount of proteinuria decreased to <0.1 g/gCr. Accompanied with elevation of plasma level of haptoglobin (from 6.8 to 99.3 mg/dl), plasma LDH and CPK decreased to their normal ranges (158 IU/l and 54 IU/l, respectively).

High tubular maximal phosphorous reabsorption (TmP)/glomerular filtration rate (GFR) (4.7 mg/dl; normal, 2.8–4.4 mg/dl) was observed in the initial analysis. Therefore, hypocalcemia resulting from parathyroid hormone (PTH) insufficiency was suspected, and treatment by calcium and vitamin D supplementation (calcium lactate, 6 g/day; calcitriol, 1 μg/day) was also started from the first day of admission. However, the serum concentrations of both 1,25(OH)$_2$ vitamin D$_3$ and intact PTH at the time of admission were found to have been 41 pg/ml (normal, 20–60 pg/ml) and 40.8 pg/ml (normal, 20–65 pg/ml), respectively. Furthermore, with normalization of the serum Ca and iP (around 9.5 mg/dl and 4.0 mg/dl, respectively), the serum intact PTH concentration decreased to 16.5 pg/ml, and the amount of urinary calcium excretion increased to 130 mg/gCr (from 20 mg/gCr at the time of hypocalcemia). Therefore, the supplementation therapy was stopped. The serum Ca and iP was kept around 8.5 mg/dl and 3.0 mg/dl without any supplementation therapy afterward, as shown in the clinical course of the present case (Fig. 1). The TmP/GFR also decreased to 3.5 mg/dl.

Discussion

In the present case, hypocalcemia with clinical symptoms (Trousseau's sign, Chvostek's sign, and elongated QTc interval on electrocardiogram) was noted in a patient suffering from severe hypertension. Because hypotension is generally seen in hypocalcemia, it is difficult to consider hypocalcemia as the primary abnormality in patients with hypertension [8]. Hypertensive organ damage is thought to be the primary abnormality in the present case, although hypocalcemia can also cause organ damage [8–10].

The kidney is the main regulatory organ of iP homeostasis [2–4]. Because about 80%–90% of the serum iP is filtered at the glomerulus, increased serum iP enhances urinary iP excretion [2]. Therefore, iP loads usually do not result in

hyperphosphatemia so long as the glomerular filtration ratio (GFR) is not severely impaired. Supporting this notion, in the reported cases of rhabdomyolysis, hyperphosphatemia was accompanied with reduced ability of the kidney to excrete iP loads; the serum iP concentration was about 7.0 mg/dl with renal failure, whereas it was 3.0–4.0 mg/dl without renal failure [11,12]. In the present case, GFR was decreased but not severely impaired (the residual CCr was around 50 ml/min). However, the amount of the urinary iP excretion was only 420 mg/gCr (less than the normal amount of 600–800 mg/day) even at the time of hyperphosphatemia, which indicated that the urinary iP excretion decreased rather than increased in spite of hyperphosphatemia [2,3].

In the kidney, iP filtered at the glomerulus is reabsorbed by the renal tubules [2–4]. The renal tubular iP reabsorption can vary over a wide range according to the amount of iP load and is predominantly regulated by PTH; PTH decreases renal tubular iP reabsorption and increases urinary iP excretion [2,3]. Therefore, with preserved renal function, hypoparathyroidism can be associated with hyperphosphatemia [2]. In the present case, hypocalcemia was also observed in association with hyperphosphatemia. The serum PTH, which is highly dependent on the serum Ca concentration, could have increased [13]. Therefore, the serum PTH, which was within its normal range but not increased, indicated impaired parathyroid reserve, because the maximum secretory rate represents the reserve of the parathyroid's capacity to respond to hypocalcemia [14].

In the present case, the serum PTH decreased as the serum Ca was increased by supplementation therapy, and the autotransplanted parathyroid was thought to be functional. The parathyroid could respond to the change of serum Ca and iP in the usual range, but it could not sufficiently compensate for a large amount of iP load [15]. The TmP/GFR, which was decreased by antihypertensive treatment, indicates that the parathyroid's capacity had been further decreased during the severe hypertensive state. Insufficient blood perfusion to the autotransplanted parathyroid caused by vasoconstriction could have contributed to the decreased parathyroid response to hypocalcemia. Antihypertensive treatment probably increased blood perfusion to the parathyroid by vascular dilatation [16] and allowed recovery of parathyroid response to hypocalcemia.

In summary, we have reported a case of hypocalcemia with severe hypertension and an autotransplanted parathyroid. The impaired reserve of the autotransplanted parathyroid and a large amount of iP load from hypertensive organ damages caused hypocalcemia. In the patients with impaired parathyroid reserve, appropriate supplementation therapy should be given with careful monitoring of serum Ca and iP.

References

1. Mundy GR, Guise TA (1999) Hormonal control of calcium homeostasis. Clin Chem 45:1347–1352
2. Berner YN, Shike M (1988) Consequences of phosphate imbalance. Annu Rev Nutr 8:121–148
3. Friedlander G (1996) Regulation of renal phosphate handling: recent findings. Curr Opin Nephrol Hypertens 5:316–320
4. Gaasbeek A, Meinders AE (2005) Hypophosphatemia: an update on its etiology and treatment. Am J Med 118:1094–1101
5. Arrambide K, Toto RD (1993) Tumor lysis syndrome. Semin Nephrol 13:273–280
6. Singh D, Chander V, Chopra K (2005) Rhabdomyolysis. Methods Find Exp Clin Pharmacol 27:39–48
7. Vanholder R, Sever MS, Erek E, Lameire N (2000) Rhabdomyolysis. J Am Soc Nephrol 11:1553–1561
8. Guise TA, Mundy GR (2000) Disorders of calcium metabolism. In: Seldin DW, Giebisch G (eds) The Kidney. Lippincott Williams & Wilkins, Philadelphia, pp 1811–1839
9. Akmal M (1993) Rhabdomyolysis in a patient with hypocalcemia due to hypoparathyroidism. Am J Nephrol 13:61–63
10. Kaplan NM (2002) Hypertensive crises. In: Kaplan NM (ed) Kaplan's Clinical Hypertension. Lippincott Williams & Wilkins, Philadelphia, pp 339–356
11. Akmal M, Bishop JE, Telfer N, Norman AW, Massry SG (1986) Hypocalcemia and hypercalcemia in patients with rhabdomyolysis with and without acute renal failure. J Clin Endocrinol Metab 63:137–142
12. Shieh SD, Lin YF, Lin SH, Lu KC (1995) A prospective study of calcium metabolism in exertional heat stroke with rhabdomyolysis and acute renal failure. Nephron 71:428–432
13. Brown EM (1982) PTH secretion in vivo and in vitro. Regulation by calcium and other secretagogues. Miner Electrolyte Metab 8:130–150
14. Brown EM (1983) Four-parameter model of the sigmoidal relationship between parathyroid hormone release and extracellular calcium concentration in normal and abnormal parathyroid tissue. J Clin Endocrinol Metab 56:572–581
15. Schmitt CP, Locken S, Mehls O, Veldhuis JD, Lehnert T, Ritz E, Schaefer F (2003) PTH pulsatility but not calcium sensitivity is restored after total parathyroidectomy with heterotopic autotransplantation. J Am Soc Nephrol 14:407–414
16. Hernandez-Hernandez R, Sosa-Canache B, Velasco M, Armas-Hernandez MJ, Armas-Padilla MC, Cammarata R (2002) Angiotensin II receptor antagonists role in arterial hypertension. J Hum Hypertens 16(suppl 1):S93–S99

http://www.kidney-international.org

Treatment of fibromuscular dysplasia

Kidney International (2008) **74,** 244; doi:10.1038/ki.2008.171

To the Editor: In a recent publication, Sinnamon *et al.*[1] showed the images of renal infarction caused by fibromuscular dysplasia. Although the authors stated that a satisfactory radiological result was achieved, we have some concern about the result of the percutaneous intervention.

The magnetic resonance angiogram shows a branch feeding the upper pole of the right kidney (arrowhead no. 1). However, the selective renal angiogram after the intervention does not show this branch, and the angiographic intensity of the upper pole is faint (arrowhead no. 2). We suspect stenosis of the branch for the upper pole, which would have been better if dilated. Supporting this notion, the diameter of the branch indicated by the arrowhead no. 3 is too small to be a primary branch (please compare the diameter with those of other primary branches). As the intervention in the case revealed additional branches (please compare the upper branch in Figures 3 and 5 of Sinnamon *et al.*), dilation of the branch (indicated by the arrowhead no. 3) could have revealed another branches, which might necessitate intervention.

The angiographic intensity of the lower pole after the intervention is also faint (arrowhead no. 4), and we think that the lesion indicated by the arrowhead no. 5 would have been better if dilated. The disturbance of renal perfusion by these lesions (arrowheads nos. 3 and 5) could have induced renovascular hypertension and necessitated antihypertensive treatment after intervention in the case.[2] Improvement of the renal perfusion by angioplasty for these lesions could have not only cured hypertension but also preserved more renal function.[3]

1. Sinnamon K, McNally D, Harty J. Fibromuscular dysplasia presenting as renal infarction. *Kidney Int* 2007; **72**: 1295–1296.
2. Tegtmeyer CJ, Elson J, Glass TA *et al.* Percutaneous transluminal angioplasty: the treatment of choice for renovascular hypertension due to fibromuscular dysplasia. *Radiology* 1982; **143**: 631–637.
3. Slovut DP, Olin JW. Fibromuscular dysplasia. *N Engl J Med* 2004; **350**: 1862–1871.

Masayuki Tanemoto[1], Takaaki Abe[1] and Sadayoshi Ito[1]
[1]*Division of Nephrology, Hypertension and Endocrinology, Department of Medicine, Tohoku University Graduate School of Medicine, Miyagi, Japan*
Correspondence: *Masayuki Tanemoto, Division of Nephrology, Hypertension and Endocrinology, Department of Medicine, Tohoku University Graduate School of Medicine, 1-1 Seiryo-cho, Aoba-ku, Sendai, Miyagi 980-8574, Japan. E-mail: mtanemoto-tky@umin.ac.jp*

Response to 'Treatment of fibromuscular dysplasia'

Kidney International (2008) **74,** 244; doi:10.1038/ki.2008.174

The authors would like to thank Tanemoto and colleagues[1] for their comments and for highlighting the importance of a thorough angiographic evaluation by an experienced practitioner in cases such as these. Following full assessment, other lesions, for example the lesion depicted by arrowhead no. 5, also underwent intervention. However, only a limited number of views were submitted for publication given the constraints of the journal. Following a complete review of all the images, the interventional radiology team was satisfied that a good angiographic result had been achieved. This is reflected in the patient's clinical status as she currently has good blood pressure control on a single agent and essentially normal renal function despite infarcting approximately 50% of the right kidney.

1. Tanemoto M, Abe T, Ito S. Treatment of fibromuscular dysplasia. *Kidney Int* 2008; **74**: 244.

Kim T Sinnamon[1]
[1]*Nephrology Unit, Daisy Hill Hospital, 5 Hospital Road, Newry, UK*
Correspondence: *Kim T. Sinnamon, Nephrology Unit, Daisy Hill Hospital, 5 Hospital Road, Newry BT35 8DR, UK. E-mail: kimsinnamon@msn.com*

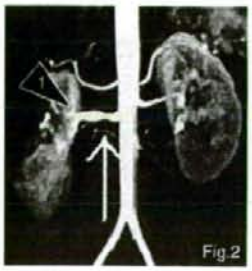

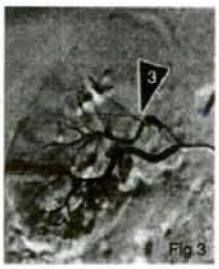

Bile acids repress E-cadherin through the induction of Snail and increase cancer invasiveness in human hepatobiliary carcinoma

Koji Fukase,[1] Hideo Ohtsuka,[1] Tohru Onogawa,[1] Hiroshi Oshio,[1] Takayuki Ii,[1] Mitsuhisa Mutoh,[1] Yu Katayose,[1] Toshiki Rikiyama,[1] Masaya Oikawa,[1] Fuyuhiko Motoi,[1] Shinichi Egawa,[1] Takaaki Abe[2] and Michiaki Unno[1,3]

[1]Department of Surgery, [2]Department of Nephrology, Endocrinology, and Vascular Medicine, Tohoku University Graduate School of Medical Science, Sendai 980-8574, Japan

(Received January 14, 2008/Revised May 13, 2008/Accepted May 23, 2008/Online publication August 7, 2008)

Although some kinds of bile acids have been implicated in colorectal cancer development, the mechanism of cancer progression remains unexplored in hepatobiliary cancer. From our personal results using complementary DNA microarray, we found that chenodeoxycholic acid (CDCA) induced Snail expression in human carcinoma cell lines derived from hepatocellular carcinoma and cholangiocarcinoma. Snail expression plays an important role in the regulation of E-cadherin and in the acquisition of invasive potential in many types of human cancers including hepatocellular carcinoma. We found that CDCA and lithocholic acid (LCA) induced Snail expression in a concentration-dependent manner and down-regulated E-cadherin expression in hepatocellular carcinoma and cholangiocarcinoma cell lines. Moreover, Snail short interference RNA (siRNA) treatment reduced the down-regulation of E-cadherin by CDCA or LCA. Luciferase analysis demonstrated that the promoter region from −111 to −24 relative to the transcriptional start site was necessary for this induction and, at least in part, nuclear factor Y (NF-Y) and stimulating protein 1 (Sp1) might be an inducer of Snail expression in response to bile acids. In addition, using an *in vitro* wound healing assay and invasion assay, we observed that CDCA and LCA induced cell migration and invasion. These results suggest that bile acids repress E-cadherin through the induction of transcription factor Snail and increase cancer invasiveness in human hepatocellular carcinoma and cholangiocarcinoma. Inhibition of this bile acid-stimulated pathway may prove useful as an adjuvant in the therapy of hepatocellular carcinoma. (*Cancer Sci* 2008; 99: 1785–1792)

Bile acids are commonly considered as physiological detergents that facilitate the absorption, transport and distribution of lipid-soluble vitamins and dietary fats. Recently, bile acids have also been shown to exert signaling activities leading to the modulation of the expression of genes involved in their own synthesis and transport.[1–4] Moreover, previous reports have indicated that bile acids can promote carcinogenesis and cancer progression, especially colon cancer, by stimulating a variety of signaling pathways.[5–7] Deoxycholic acid (DCA) has been shown to modulate p53 gene expression in a colonic adenoma cell line.[8] It was reported that the prolonged deregulated expression of activator protein-1 (AP-1) activity in colonic cells by certain bile acids contributed to tumor promotion in the colon.[9,10] Bile acids were also reported to be involved in the induction of cyclooxygenase-2 (COX-2), the secretion of matrix metalloproteinase-2 (MMP-2) and the migration of colorectal cancer cells.[11,12] Thus, some kinds of bile acids have been shown to act as tumor promoters in colon cancer. More recently, chenodeoxycholic acid (CDCA) has also been shown to activate the epidermal growth factor receptor (EGFR) and to induce COX-2 expression in hepatocellular carcinoma and cholangiocarcinoma cell lines.[13,14] These results have suggested that bile acid can also promote carcinogenesis and cancer progression in hepatocytes and cholangiocytes. However, in hepatocytes and cholangiocytes, which are always exposed to bile acids, the mechanisms of bile acid-induced carcinogenesis and cancer progression are poorly understood. Moreover, from our personal results using complementary DNA (cDNA) microarray gene expression profiling approach to identify novel genes regulated by primary bile acids (CDCA), we found that CDCA induced Snail expression in hepatocellular carcinoma and cholangiocarcinoma cell lines.

Increased cell invasion is a key phenotypic advantage of malignant cells favoring metastasis. The invasion process involves the loss of cell–cell interactions together with the gain of proteolytic and migratory properties and is often referred to as epithelial-mesenchymal transition (EMT).[15] E-cadherin is a cell–cell adhesion molecule especially expressed on the membrane of epithelial cells, and a decrease of its expression has been reported in the invasion and metastasis of cancers.[16–18] It was reported that DCA caused a significant loss of E-cadherin binding with beta-catenin, which is associated with an increase in cancer cell invasiveness as reflected by increase in the number of migrating cells.[19] The zinc finger transcriptional factor Snail represses E-cadherin transcription *in vitro* and *in vivo* by binding to E-boxes of the E-cadherin promoter. Snail was found to evoke tumorigenic and invasive properties in epithelial cells.[20] Nevertheless, the mechanisms governing the expression of human Snail are starting to be identified.[21,22]

Our purpose of this study is to identify the mechanism of Snail gene induction by bile acids and whether this induction participated in the progression of cancer cells.

Materials and Methods

Materials. Cholic acid (CA), deoxycholic acid (DCA), chenodeoxycholic acid (CDCA), lithocholic acid (LCA), ursodeoxycholic acid (UDCA), taurocholic acid (TCA), taurodeoxycholic acid (TDCA), taurochenodeoxycholic acid (TCDCA), taurolithocholic acid (TLCA), tauroursodeoxycholic acid (TUDCA), glycocholic acid (GCA), glycodeoxycholic acid (GDCA) and glycochenodeoxycholic acid (GCDCA) were obtained from Sigma Chemical (St. Louis, MO, USA), glycolithocholic acid (GLCA) was obtained from Calbiochem (San Diego, CA, USA) and glycoursodeoxycholic acid (GUDCA) was obtained from Mitsubishi Pharma Corporation (Osaka, Japan), and all of the

[3]To whom correspondence should be addressed.
E-mail: m_unno@surg1.med.tohoku.ac.jp

doi: 10.1111/j.1349-7006.2008.00898.x

bile acids were maintained as 100-mM stock solutions in dimethyl sulfoxide (DMSO). The stock solution was stored at −20°C. Mouse monoclonal anti-E-cadherin antibody (G-10), goat polyclonal antiactin antibody (I-19) and horseradish peroxidase (HRP)-linked antibody (goat antimouse for E-cadherin; donkey antigoat for actin) were purchased from Santa Cruz Biotechnology, Inc (Santa Cruz, CA, USA).

Cell culture and treatment. The THLE-3 (American Type Culture Collection [ATCC], Bethesda, MD, USA), which was derived from human primary normal liver cells[23] were cultured in BEGM® BulletKit® (Clonetic corp, MD, USA) supplemented with 10% dialyzed fetal bovine serum (FBS) (Invitrogen, Carlsbad, CA, USA), 5 ng/mL epidermal growth factor (EGF), and 70 ng/mL phosphoethanolamine. Human tumor-derived cells, Hep3B hepatocellular carcinoma and HuCCT-1 cholangiocarcinoma, were cultured in Roswell Park Memorial Institute medium (RPMI)-1640 (Sigma Chemical) supplemented with 10% dialyzed FBS, 100 mg/mL penicillin, and 100 U/mL streptomycin. The cells were maintained at 37°C in a humidified atmosphere of 5% CO_2. The cell culture was passed every three or four days.

Microarray. AceGene (Human oligo chip 30K, subset A; DNA Chip Research Inc. and Hitachi Software Engineering, Yokohama, Japan) containing 10 000 genes was used for mRNA expression profiling. (The protocol is available at http://www.dna-chip.co.jp/thesis/AceGeneProtocol.pdf.) Four μg of total RNA was amplified with an Amino Allyl MessageAmp aRNA kit (Ambion, Austin, TX, USA). Amino-allyl-labeled cRNA was purified and then 5 μg of cRNA was labeled with Cy5 Mono-reactive Dye (Amersham Biosciences Inc., Tokyo, Japan) or Cy3 Mono-reactive Dye (Amersham Biosciences Inc.), according to the protocol of Hitachi Software Engineering. The arrays were scanned using a GenePix 4000B microarray scanner (Axon Instruments Inc., Union City, CA, USA).

Data were obtained from quadruplicates of each cell lines. The digitized image data were processed using GenePix Pro 4.1 software (Axon Instruments). The result files were imported into the GeneSpring 6.1 software (Silicon Genetics, Redwood City, CA, USA) and analyzed for gene expression differences. Data were normalized using per-spot and per-chip intensity dependent (Lowess) normalization. The Cross Gene Error model was activated and based on replicates. To find differentially expressed genes, one-sample *t*-tests and Benjamini and Hochberg false discovery rate multiple testing corrections were performed at 95% confidence levels on log transformed data.

Quantitative real-time reverse transcription (RT)–polymerase chain reaction (PCR). The cells were treated with bile acids or vehicle (DMSO) for 24 h. Then, total RNA was isolated using TRIzol (Invitrogen) following standard procedures. cDNA was then synthesized from 4 μg total RNA, using the SuperScript III First-Strand Synthesis System for RT-PCR (Invitrogen) with oligo dT primer according to the manufacturer's instructions. The primer sequences were as fellows. For human Snail, forward: 5′-TCT AAT CCA GAG TTT ACC TTC CAG C-3′: reverse: 5′-AGA TGA GCA TTG GCA GCG A-3′. For human E-cadherin, forward: 5′-AGA ACG CAT TGC CAC ATA CAC TCT C-3′; reverse: 5′-CGG TTA CCG TGA TCA AAA TCT CCA-3′. The PCR reactions were carried out in a 25-μL volume containing 200 nM of each primer and 1 × QuantiTect SYBR Green PCR master mix (QIAGEN, Valencia, CA, USA). Real-time PCR was performed on the ABI PRISM 7700 Sequence Detection System (PE Applied Biosystems) using the parameters recommended by the manufacturer (2 min at 50°C, 10 min at 95°C and 40 cycles of 95°C for 15 s and 62°C for 20 s). Each PCR reaction was performed in quadruplicate. The mRNA expression levels for all samples were normalized to the levels for the housekeeping gene *GAPDH*.

Plasmid construction. The human Snail promoter 5′ flanking region[22] from −1824–1866 was amplified by PCR from human genomic DNA (Clontech Laboratories, Inc., Palo Alto, CA, USA) with the forward primer 5′-CGT *GAA GCT T*TA GGA GCA AGA GAC GTA G-3′ (−1834 to −1807) and the reverse primer 5′-GTC *GAA GCT T*TG GGG TCG CCG ATT-3′.[76,53] For cloning purposes, a *Hin*dIII site was added to both primers. The PCR product was digested with *Hin*dIII, gel-isolated and subcloned into the multiple cloning site of the pGL3–Basic Vector (Promega, Madison, WI, USA). The 5′ deletion mutants were generated by PCR and inserted into pGL3–Basic Vector. The forward primers were modified to contain a *Bgl*II restriction site. The sequences of primers were as follows: −966/66 forward: 5′-AGC *AGA TCT* GAC CCC TCC GG-3′ (−975 to −956), −339/66 forward: 5′-CTC *AGA TCT* CCG GGC GCT GA-3′ (−348 to −329), −111/66 forward: 5′-CGG *AGA TCT* GCC TCC GAT TGG C-3′ (−120 to −99), −66/66 forward: 5′-CAG *AGA TCT* CCC CGC CCC TC-3′ (−75 to −56), −24/66 forward: 5′-GAG T*AG ATC T*GG GAG TTG GCG GC-3′ (−34 to −13) and reverse (common): 5′-GTC *GAA GCT T*TG GGG TCG CCG ATT-3′ (76 to 53). The PCR product was digested with *Bgl*II and *Hin*dIII and subcloned into the multiple cloning site of the pGL3–Basic Vector. All reporter constructs were sequenced to confirm the correct sequence.

Site-directed mutagenesis. The mutants were generated from the −1824/66 Snail pGL3 construct using the QuickChange Site-Directed Mutagenesis kit (Stratagene). The following oligonucleotides were used as primers: 5′-CTT CGG CGG AGA CGA GCC TCC *GGT CCG* CGC GGA GGT GAC AAA GGG GCG-3′ and 5′-CGC CCC TTT GTC ACC TCC GCG C*GG* A*CC* GGA GGC TCG TCT CCG CCG AAG-3′ for mutation in the nuclear factor Y (NF-Y) binding site, 5′-GAT TGG CGC GGA GG*C CCG* AAA GGG GCG TGG CAG-3′ and 5′-CTG CCA CGC CCC TTT *CGG G*CC TCC GCG CCA ATC-3′ for mutation in the AP-1 binding site, and 5′-GCA GAT AAG GCC CC*C AAA* CTC CCA CCC CCC AC-3′ and 5′-GTG GGG GGT GGG AG*T TTG* GGG GCC TTA TCT GC-3′ for mutation in the stimulating protein 1 (Sp1) binding site. The presence of mutations was verified by sequencing.

Transient transfection and luciferase assay. DNA constructs were transiently transfected into cells using LipofectAMINE 2000 Reagent (Invitrogen). Twenty-four hours before transfection, Hep3B cells were subcultured in 24-well plates so that they would be at 70% confluence on the following day. Transfections were optimized for the amounts of DNA and LipofectAMINE per well culture as follows: 0.3 μg of reporter plasmids; 10 ng of pRL-TK vector (Promega) as an internal control; and 2 μL of LipofectAMINE Reagent. 24 h after the transfection, the bile acid was added to the cell culture media and the cells were incubated for another 24 h. Luciferase assays were performed with the dual-luciferase reporter assay system (Promega). All reported firefly luciferase values were normalized for transfection efficiency using the pRL-TK, Renilla-luciferase value. Graphs are representative for one of two experiments, each performed in quadruplicate.

Western blot analysis. The cells were treated with bile acids or vehicle (DMSO) for 24 h. Whole-cell lysates were prepared and aliquots of 40 μg of protein lysates were applied for the sodium dodecyl sulfate–polyacrylamide gel electrophoresis (SDS-PAGE). Blots were probed with antibodies against E-cadherin diluted 1:200 or actin diluted 1:500. Both were stained using secondary HRP-conjugated antibodies diluted 1:1000 (goat antimouse for E-cadherin and donkey antigoat for actin).

RNA interference. siGENOME SMARTpool reagent for Human Snail and siCONTROL Non-Targeting siRNA Pool were obtained from Dharmacon, Inc (Lafayette, CO, USA). Short interference RNA (siRNA) was transiently transfected into cells using LipofectAMINE 2000 Reagent. Transfections were optimized for the amounts of siRNA, and LipofectAMINE per well culture

doi: 10.1111/j.1349-7006.2008.00898.x

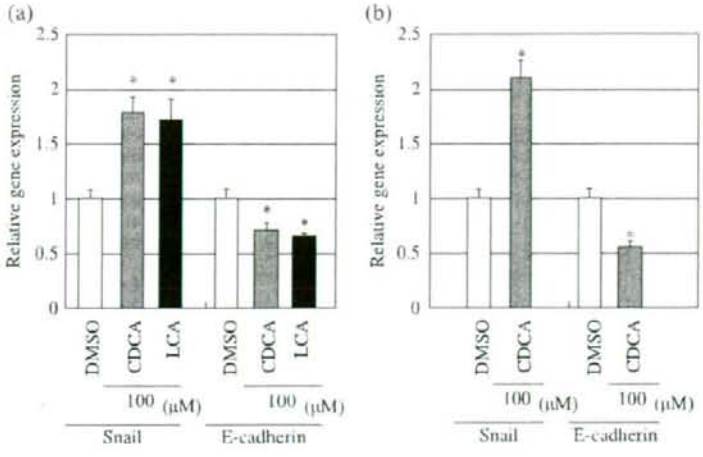

Fig. 1. Chenodeoxycholic acid (CDCA) and lithocholic acid (LCA) induced expression of Snail mRNA and reduced expression of E-cadherin mRNA. Cells were incubated with 100 μM of CDCA or LCA for 24 h. Then, total RNA was isolated and quantitative real-time reverse transcription–polymerase chain reaction (RT-PCR) was performed. (a) Hep3B cells were treated with 100 μM of CDCA or LCA. (b) HuCCT-1 cells were treated with 100 μM of CDCA. Values for each gene were normalized to values obtained for GAPDH. *Y*-axis represents a ratio for control (dimethyl sulfoxide [DMSO]). The data show the mean ± SD. *Significant difference ($P < 0.01$) from the respective control value.

as follows: 200 ng of siRNA and 4 μL of LipofectAMINE 2000 Reagent. The final concentration of siRNA used in each experiment was 100 nM.

***In vitro* wound healing assay.** Cells were seeded in 24-well culture plates at 1×10^5 cells/well. After 12 h, the cells were pretreated with bile acid for 24 h before wound formation. The *in vitro* 'scratch' wounds were created by scraping the confluent cell monolayer with a sterile pipette tip. The cells were incubated with bile acid. After 6 h and 12 h, the cells were fixed with 100% methyl alcohol and stained with 0.5% solution of crystal violet and the distance of the wound closure (compared with control at t = 0 h) was measured in three independent wound sites per group. Relative cell motility was calculated as the percentage of the remaining cell-free area compared with the area of the initial wound. Values from at least three independent experiments were pooled and expressed as mean ± standard deviation (SD).

Invasion assay. The cell invasion ability was determined using a BD Matrigel invasion chamber 24-well Plate (BD Biosciences, Bedford, MA, USA), in which the chamber membrane filter (8 μm pore size) was coated with BD Matrigel Basement Membrane Matrix (BD Biosciences). The upper chamber was loaded with 2×10^4 cells in 0.2 mL of serum-free medium with bile acid, and the lower chamber was filled with 0.7 mL of serum-containing medium with bile acid. After 48 h, invading cells on the lower surface of the membrane were washed in phosphate-buffered saline (PBS), fixed with 100% methyl alcohol and stained with 0.5% solution of crystal violet. The invading cells were counted under a microscope in six randomly selected fields for each membrane filter (×200). Each sample was assayed in duplicate in at least two independent experiments.

Data analysis. The obtained values are expressed as the mean ± SD. The data from different treated groups were compared by Welch *t*-test. *P*-values of <0.01 were considered to be statistically significant.

Results

Gene expression profiles induced by CDCA using cDNA microarray. To identify the changes in gene expression induced by CDCA, THLE-3, Hep3B and HuCCT-1 were treated with 100 μM of CDCA for 24 h. The cells treated with 0.1% DMSO were used as the control. Total RNA was isolated and gene expression profiling was performed by cDNA microarray using the AceGene (Human oligo chip 30K, subset A). The relative transcript abundance was expressed as Cy5/Cy3 ratios of signal intensities after background subtraction in each channel. Data analysis and quality control procedures are described in detail in section of Materials and methods. Seventy-six genes were up-regulated in the THLE-3, 119 genes in the Hep3B and 53 genes in the HuCCT-1. One-hundred and nineteen genes were down-regulated in the THLE-3, 97 genes in the Hep3B and 18 genes in the HuCCT-1. The Venn diagrams depict the number of overlapping and non-overlapping genes (Fig. 1). The overlapping genes in all cell lines were listed as the common CDCA-induced up- or down-regulated genes (see Suppl. Table S1). In addition, E-cadherin, which is a target gene of Snail, showed significant down regulation after 24-h CDCA treatment in Hep3B and HuCCT-1 (fold change; 0.73 and 0.62, *P*-value; 0.003 and 0.037, respectively). However, the spot for E-cadherin in several hybridizations of THLE-3 was detected as a missing spot and E-cadherin was eliminated from further analysis.

CDCA- and LCA-induced expression of Snail mRNA and reduced expression of E-cadherin mRNA. To investigate alteration in the expression of Snail mRNA and E-cadherin mRNA by bile acids, quantitative real-time RT-PCR was performed. Hep3B and HuCCT-1 cells showed induced expression of Snail and reduced expression of E-cadherin by 100 μM of CDCA or LCA (Fig. 1). The relative Snail gene expression resulted in an approximately 1.8-fold increase in the Hep3B cells and about 2.2-fold increase in the HuCCT-1 cells, whereas the relative E-cadherin expression resulted in a 0.7-fold decrease in the Hep3B cells and about 0.5-fold decrease in the HuCCT-1 cells. These results demonstrated that E-cadherin expression was inversely correlated with the expression of Snail, suggesting that up-regulation of Snail by bile acids might be involved in the down-regulation of E-cadherin in hepatocellular carcinoma.

CDCA and LCA treatment induce Snail promoter activity in a concentration-dependent manner. To determine whether the increased mRNA levels of Snail are associated with increased transcriptional activity, luciferase assays were performed. Hep3B cells were cotransfected with −1824/66 Snail pGL3 constructs and pRL-TK vector and treated with 100 μM of various bile acids for 24 h. CDCA resulted in an approximately 2-fold increase in luciferase activity compared with the control (DMSO). Furthermore LCA resulted in an approximately 3-fold increase in luciferase activity compared with the control (DMSO). In contrast, the other free bile acids, glycine-conjugated and taurine-conjugated bile acids, caused no change

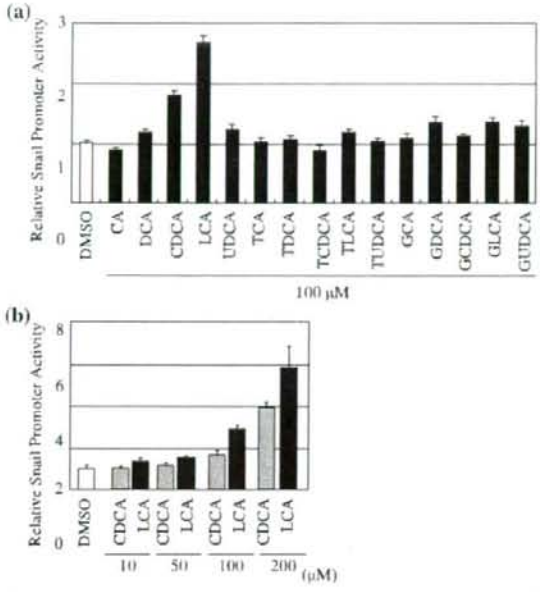

Fig. 2. Chenodeoxycholic acid (CDCA) and lithocholic acid (LCA) increased Snail promoter activities in a concentration-dependent manner. To investigate the effects of bile acids on the transcription of the Snail gene, 0.3 μg of the −1824/66 Snail pGL3 constructs and 10 ng of pRL-TK vector were cotransfected into Hep3B cells. After 24 h, the bile acid was added to the cell culture media and the cells were incubated for 24 h. All reported firefly luciferase values were normalized for transfection efficiency using the pRL-TK, Renilla-luciferase value. *Y*-axis represents the ratio for control (dimethyl sulfoxide [DMSO]). (a) The transfected cells treated with the various bile acids. The transfected cells treated with increasing amounts of (b) The transfected cells treated with CDCA or LCA at the concentration of 10–200 μM. The data show the mean ± SD of quadruplicate assay.

in luciferase activity (Fig. 2a). Treatment with CDCA or LCA resulted in a concentration-dependent increase in Snail promoter activities (Fig. 2b).

NF-Y and Sp-1 binding sites of Snail promoter are responsible for CDCA and LCA. To define the regulatory sequences required for the transcription of the Snail gene, Hep3B cells were cotransfected with a series of 5′-deleted Snail pGL3 constructs and pRL-TK vector and treated with 100 μM LCA for 24 h. In non-LCA-treated cells, deletion of nucleotides −1824 to −111 had no significant effect on the luciferase activity. However, deletion to nucleotide −66 resulted in significantly lower luciferase activity compared with that seen with Snail −1824/66-Luc. Deletion to nucleotide −24 resulted in complete loss of the luciferase activity. In contrast, in LCA-treated cells, luciferase activities were significantly higher than in untreated control cells and gradual deletion of the 5′ sequences from nucleotides −1875 to −111 resulted in no significant difference in the luciferase activity (Fig. 3a). The maximal activity was seen with Snail −111/66-Luc. On further deletion to nucleotide −66, the luciferase activity fell to 47% of the maximal activity ($P < 0.01$). Deletion to nucleotide −24 resulted in complete loss of the luciferase activity. These results show that the region from nucleotide −111 to −24 is required for the maximal expression of Snail in Hep3B cells, both in the presence and absence of LCA.

To confirm which potential binding site from −111 to −24 was important for the induction of the Snail gene, we measured the luciferase activity by site-directed mutagenesis. The vector mutated in the AP-1 binding site showed no significant change compared with the wild-type construct. The vector mutated in the NF-Y or Sp1 binding site resulted in a marked decrease of the luciferase activity compared with the wild-type construct in the both absence and presence of LCA (Fig. 3b). However, the luciferase activity of the vector mutated in the NF-Y or Sp1 binding site treated with LCA still remained about 1.9- or 1.7-fold higher than the activity of untreated cells, respectively. These results suggested that the NF-Y and Sp1 binding sites were required for the basal activity of the Snail promoter, which is at least in part an inducer of Snail expression in response to bile acids.

Effects of E-cadherin protein level and of subcellular localization of E-cadherin by bile acid. To investigate alteration of subcellular localization of E-cadherin by bile acid, immunofluorescence experiments with antibody to E-cadherin were performed. Confocal microscopic studies revealed no significant difference in E-cadherin protein pattern of subcellular distribution between Hep3B treated with DMSO, with 100 μM CDCA and with 100 μM LCA. In all treated cells, E-cadherin staining was localized at areas of cell–cell contact. Moreover, in CDCA- and LCA-treated cells, it seemed that E-cadherin showed slightly weak staining, while strong membranous staining was observed in DMSO treated cells. Then, to verify the alteration in the expression of E-cadherin protein by bile acid, Western blotting was performed. Treatment with CDCA or LCA resulted in a concentration-dependent decrease in E-cadherin protein expression. The expression of E-cadherin in LCA-treated cells was lower than that in CDCA-treated cells (Fig. 4b). Western blotting analyzes confirmed the immunofluorescence results.

Snail expression modulates E-cadherin levels. To examine whether the increased Snail expression by CDCA and LCA led to reduced E-cadherin levels, we used RNA interference to reduce the Snail expression in Hep3B cells. Transfection with Snail siRNA resulted in an 80% reduction of the Snail mRNA levels compared with Hep3B cells transfected with Non-Targeting siRNA (Fig. 5a). Concomitantly, transfection with Snail siRNA also led to a 55% increase in the levels of E-cadherin mRNA. Transfection with Non-Targeting siRNA treated with 100 μM of CDCA or LCA showed 22% or 47% reductions in the E-cadherin mRNA levels, respectively, compared with Hep3B cells treated with DMSO. However, Snail siRNA treatment reduced the down-regulation of E-cadherin (about 30% of that by transfection with Non-Targeting siRNA) by 100 μM of CDCA or LCA (Fig. 5b). These results demonstrated that CDCA and LCA activated the Snail signaling pathway and reduced the E-cadherin levels in hepatocellular carcinoma cell lines.

CDCA and LCA induces cell migration and invasion. To test whether the increased Snail expression by CDCA or LCA induced cell migration and invasion, cell motility and invasiveness were assessed using an *in vitro* wound healing assay and cell invasion assay. Our results showed that CDCA and LCA induced the ability of Hep3B cells to close the wound (Fig. 6a). MTS assay showed that the cell growth of Hep3B was not affected by concentrations of CDCA or LCA lower than 100 μM as compared with control (data not shown). The increased motility induced by CDCA and LCA treatment was not the result of increased cell proliferation. Invasion assays were carried out using Matrigel-coated transwell culture chambers. Hep3B cells treated with CDCA showed significantly increased cell invasion compared with cells treated with vehicle. Furthermore, cells treated with LCA exhibited markedly increased cell invasion compared with the cells treated with vehicle (Fig. 6b). Transfection with Snail siRNA resulted in marked decreases in cell invasion compared with Hep3B cells transfected with Non-Targeting siRNA. Moreover, there was a loss of the increase in cell invasion induced by CDCA and LCA (Fig. 6c).

doi: 10.1111/j.1349-7006.2008.00898.x

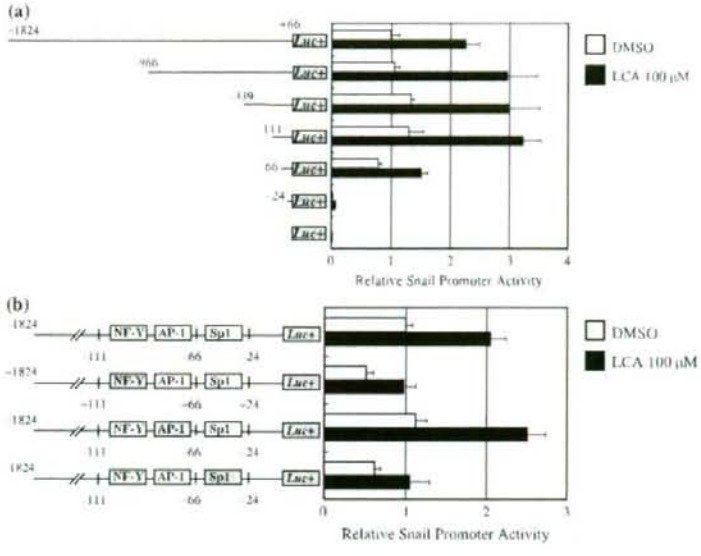

Fig. 3. Deletion and mutagenesis analyzes of Snail promoter. 0.3 μg of each construct and 10 ng of pRL-TK vector were cotransfected into Hep3B cells. After 24 h, the bile acid was added to the cell culture media and the cells were incubated for 24 h. All reported firefly luciferase values were normalized for transfection efficiency using the pRL-TK, Renilla-luciferase value activity and are shown as the relative activity compared to that for -1824/66 Snail pGL3 constructs treated with dimethyl sulfoxide (DMSO). The data show the mean ± SD of quadruplicate assay. (a) Deletion analysis of Snail promoter for the induction by LCA. (b) Effect of mutagenesis in NF-Y, AP-1 and Sp1 binding site on Snail promoter activity. The mutant promoter constructs used are schematically drawn.

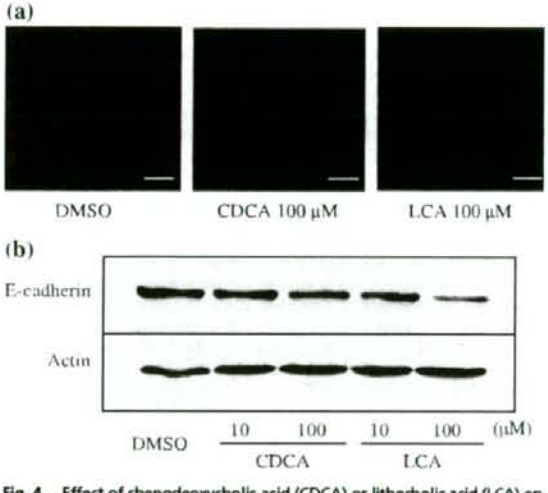

Fig. 4. Effect of chenodeoxycholic acid (CDCA) or lithocholic acid (LCA) on E-cadherin protein expression and subcellular distribution. Hep3B cells were incubated with bile acids or dimethyl sulfoxide (DMSO) for 24 h (a) Hep3B cells were fixed and probed with an anti-E-cadherin antibody followed by Alexa Fluor 488-conjugated antimouse secondary antibody. Immunofluorescence showed the localization of E-cadherin proteins (green fluorescence). Panel (left); DMSO (middle); CDCA 100 μM (right); LCA 100 μM treatmrnt. Bar, 20 μm (b) Protein levels were determined by Western blotting of whole cell extracts using mouse monoclonal anti-E-cadherin antibody. The expression of actin was analyzed in the same samples as a control for the amount of protein present in each sample.

Discussion

Bile acids are natural detergents synthesized in the liver. High levels of certain bile acids, however, are known to promote carcinogenesis and cancer progression by stimulating a variety of signaling pathways.[5-7] The mechanisms of the tumor-promoting actions of bile acids remain poorly understood.

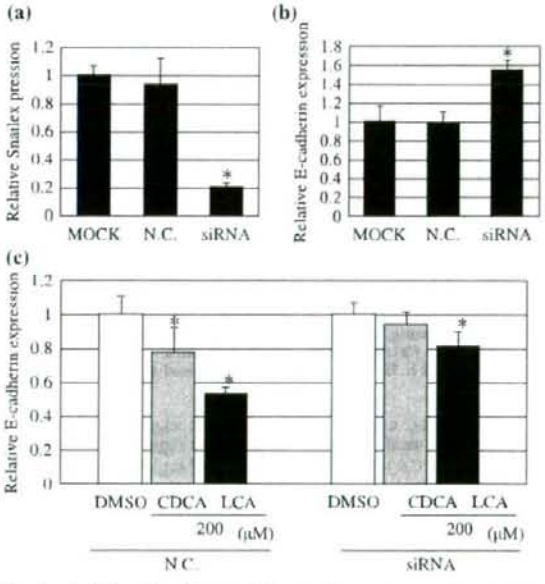

Fig. 5. Snail short interference RNA (siRNA) treatment reduces down-regulation of E-cadherin by chenodeoxycholic acid (CDCA) or lithocholic acid (LCA). 200 ng of siRNA (final concentration: 100 nM) were transfected into Hep3B cells. After 72 h total RNA was isolated and quantitative real-time reverse transcription–polymerase chain reaction (RT-PCR) was performed. (a) The mRNA expression level of Snail. (b) The mRNA expression level of E-cadherin. Mock: treated with only transfection reagent and N.C.: Non-Targeting siRNA used as negative control. *Significant difference ($P < 0.01$) from N.C. (c) After transfection, Hep3B cells were incubated for 48 h and then cells were incubated with CDCA or LCA for 24 h. Total RNA was isolated. As a control, the same volume of dimethyl sulfoxide (DMSO) was used. The data show the mean ± SD. *Significant difference ($P < 0.01$) from the respective control value.

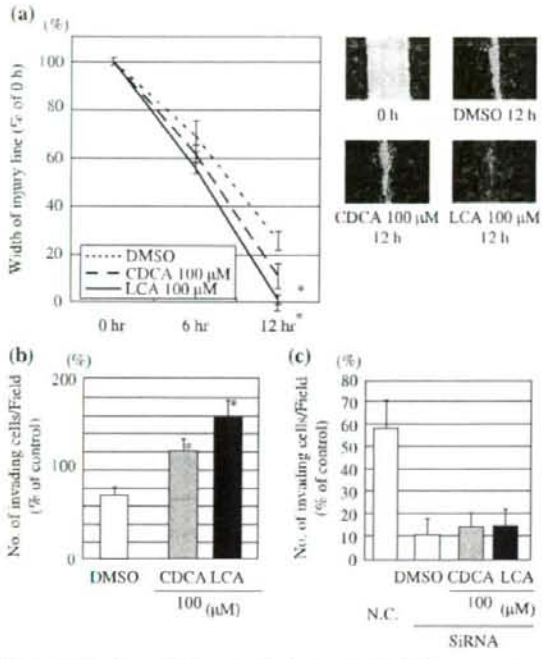

Fig. 6. Chenodeoxycholic acid (CDCA) and lithocholic acid (LCA) induce cell migration. (a) The motility behavior of bile acid treated cells was analyzed in an *in vitro* wound model. Confluent cultures of Hep3B cells treated with bile acids were gently scratched with a pipette tip to produce a wound. Quantitative analysis was performed as described in Materials and methods. Data are mean ± SD. *Significant different ($P < 0.01$) from the respective control (dimethyl sulfoxide [DMSO]). (right panels) Photographs of cell migration were taken immediately after the incision and after 12 h. (b) The cell invasion assays were performed as described in Materials and methods. The invading cells were counted under the microscope in 6 randomly selected fields for each membrane filter (×200). Each sample was assayed in duplicate in at least two independent experiments. Data are mean ± SD. *Significant difference ($P < 0.01$) from the respective control (DMSO). (c) The cell invasion assays were performed using Snail knocked down cells. Before plating, 200 ng of short interference RNA (siRNA) (final concentration: 100 nM) were transfected into Hep3B cells and incubated for 72 h. N.C.: Non-Targeting siRNA used as negative control.

In this study, a DNA microarray gene expression profiling approach was used to identify novel genes regulated by primary bile acids (CDCA) in hepatocytes and cholangiocytes. From this screening, several genes were found to be up- or down-regulated in the presence of CDCA. Snail was found to be up-regulated and E-cadherin, a target gene of Snail, was found to be down-regulated by the addition of CDCA. This is the first report that bile acids induced Snail.

Bile acids have been shown to modulate gene expression by regulating its promoter activity. The bile acids were reported to bind to the nuclear hormone receptors including farnesoid X-activated receptor (FXR).[2,24-27] Some kinds of nuclear hormone receptors can recognize bile acid response element (BARE) such as direct repeat, inverted repeat and everted repeat.[28] In addition, bile acids can also activate NF-kappa B and AP-1.[10,29] In this study, we revealed that several kinds of bile acids were able to induce Snail expression by activating its promoter activity. The luciferase assays showed treatment with 100 μM of CDCA or LCA resulted in 2–3-fold increase in Snail promoter activities. The deletion mutant series for the Snail promoter revealed that 111 bp upstream of the transcription start site of the Snail gene was essential for the maximal promoter activity in both LCA-treated and LCA-untreated Hep3B cells. By sequence analysis of the 5′ flanking region of Snail gene, potential binding sites for NF-Y, AP-1 and Sp1 were identified on the 111 bp upstream region.

The Sp1 family of proteins is ubiquitously expressed in many tissues. They have versatile functions and are involved in cell cycle or differentiation.[30] Early studies indicated that Sp1 was responsible for recruiting TATA-binding protein and guiding transcriptional initiation at promoters without a TATA box.[31-33] Sp1 proteins are known to interact with general transcription factors and are involved in the assembly of general transcriptional complexes. In addition to their function as general transcriptional activators, recent studies indicate Sp1 proteins also interact with many unique transcription factors and synergistically stimulate the genes involved in cholesterol and fatty acids synthesis.[34,35] RAR, a well-known nuclear receptor that heterodimerizes with RXR and binds to RAR-responsive element to regulate gene expression, was reported to modulate Sp1 transcriptional activity on GC-rich promoters through direct interaction between the two proteins.[36,37] As shown in Fig. 2(a), hydrophobic bile acids, CDCA and LCA could activate the promoter activity of Snail, whereas hydrophilic bile acids, taurin- or glycin- conjugated bile acids could never activate Snail promoter activity. In general, unconjugated hydrophobic bile acids have higher affinity with nuclear receptors such as FXR than conjugated hydrophilic bile acids. It is speculated that CDCA or LCA, which might be able to enter the cell by passive diffusion through the plasma membrane of the cancer cell, directly activate the nuclear receptors and modulate the Sp1 transcriptional activity on the Snail promoter.

The NF-Y is known as a ubiquitous heterotrimeric transcription factor that consist of NF-YA, NF-YB and NF-YC subunits.[38,39] Functional analysis has shown that NF-Y is crucial for transcriptional activation and reinitiation on genes that lack a TATA-box.[33,40] In addition, it was suggested that NF-Y could functionally interact with Sp1 and synergistically regulate promoter activity. Wright *et al.* demonstrated that the half-life of either NF-Y or Sp1 binding is dramatically increased when both transcriptional factors are bound to the proximal promoter of the major histocompatibility complex class II-associated invariant chain gene.[41] Liang *et al.* reported that the type-A natriuretic peptide receptor gene transcription was regulated through functional interactions of NF-1 and Sp1.[42] The present study showed that mutations on NF-Y or Sp1 binding sites in the Snail promoter markedly reduced transcriptional activity, possibly suggesting that the transcriptional activity of Snail was regulated by the functional interaction of NF-Y and Sp1. In addition, the promoter activity of mutant on NF-Y or Sp1 was higher compared with the minimal activation level observed with deletion to nucleotide –24, indicating that either NF-Y or Sp1 are indispensable for the transcription of Snail. We also demonstrated that the promoter activity of the 111 bp upstream region was dramatically up-regulated by CDCA or LCA, suggesting that these bile acids regulate the transcriptional activity of Snail gene by interacting with putative NF-Y and Sp1 binding sites. 100 μM of LCA could up-regulate the promoter activity of both mutant on NF-1 and mutant on Sp1. It was suggested that these bile acids activate both Sp1 and NF-Y. The effect of these bile acids on the activation of NF-Y or Sp1 remains to be explored. To clarify the molecular mechanism of transcriptional regulation of Snail gene by bile acids will require further study.

In this present study, we revealed that the expression of E-cadherin was decreased in CDCA- or LCA-treated Hep3B cells. Alterations affecting cell adhesion molecules are considered to play a critical role in the invasive process. The cell–cell adhesion molecule E-cadherin has been shown to execute important

doi: 10.1111/j.1349-7006.2008.00898.x

functions in embryogenesis and tissue architecture by forming intercellular junction complexes and establishing cell polarization.[43] Loss of E-cadherin results in dedifferentiation, invasiveness and lymph node or distant metastasis in a variety of human neoplasms, including hepatocellular carcinoma.[16–18,44] Recently, the up-regulation of the transcription factor Snail was reported to mediate significant negative regulation of E-cadherin expression.[20,45] The Snail mRNA levels have been reported to be independently correlated with capsular invasion in hepatocellular carcinoma tissues.[46,47] Moreover, transfection of Snail in epithelial cells decreases E-cadherin levels and induces changes resembling EMT.[20,45] Interference with Snail expression leads to increased levels of E-cadherin.[21,45,48] The results from our present study showed that Snail expression was induced and E-cadherin expression was reduced by CDCA or LCA. Moreover, it was revealed that these bile acids could never reduce the expression of E-cadherin in Snail knocked down Hep3B cells. Together with these results, it is suggested that CDCA and LCA activate the Snail signaling pathway and reduce the expression of E-cadherin in hepatocellular carcinoma cell lines. To address the hypothesis that Snail expression causes increased cancer invasion, the invasion activity was assessed using an *in vitro* wound healing assay and invasion assay. The invasive activity in Hep3B treated with 100 μM of CDCA or LCA was significantly increased compared with vehicle. Transfection with Snail siRNA resulted in marked decreases in cell invasion and a loss of the increase in cell invasion induced by CDCA and LCA. These results suggest that CDCA and LCA induce the expression of Snail gene, and as a consequence, promote invasiveness of the hepatocellular carcinoma cells. In the presented experiments, CDCA and LCA were applied at the concentration of 100 μM. Most of the biliary bile acids are conjugated and 100 μM of CDCA or LCA is excessively high as a concentration of physiological condition. However, in a pathological condition such as obstructive jaundice, hepatocellular carcinoma cells or cholangiocarcinoma, cells are probably exposed to these high concentrations of bile acids.

In summary, we found that CDCA and LCA positively regulate the transcriptional activity of the Snail gene. We showed that CDCA and LCA could activate the transcription of the Snail gene. Our data suggested that both Sp1 and NF-Y are essential for this bile-acid-induced transcriptional activity. We revealed that CDCA or LCA could down-regulate the expression of E-cadherin by stimulating the Snail pathway and, as a consequence, these bile acids could promote cancer cell invasiveness. Hence, we conclude that CDCA and LCA are a novel inducer of Snail expression. It is suggested that CDCA and LCA play some role in promoting cancer invasiveness by stimulating the Snail pathway in hepatocelluler carcinoma. It is also suggested that inhibition of this bile-acid-stimulated Snail pathway may prove useful as an adjuvant in therapy for hepatocellular carcinoma.

Grant support

This study was supported by a Grant-in Aid for Scientific Research from the Ministry of Education, Culture, Sports, Science and Technology of Japan and Sagawa Foundation.

References

1 Pandak WM, Li YC, Chiang JY *et al.* Regulation of cholesterol 7 alpha-hydroxylase mRNA and transcriptional activity by taurocholate and cholesterol in the chronic biliary diverted rat. *J Biol Chem* 1991; **266**: 3416–21.
2 Wang H, Chen J, Hollister K, Sowers LC, Forman BM. Endogenous bile acids are ligands for the nuclear receptor FXR/BAR. *Mol Cell* 1999; **3**: 543–53.
3 Grober J, Zaghini I, Fujii H *et al.* Identification of a bile acid-responsive element in the human ileal bile acid-binding protein gene. Involvement of the farnesoid X receptor/9-cis-retinoic acid receptor heterodimer. *J Biol Chem* 1999; **274**: 29749–54.
4 Pineda Torra I, Claudel T, Duval C, Kosykh V, Fruchart JC, Staels B. Bile acids induce the expression of the human peroxisome proliferator-activated receptor alpha gene via activation of the farnesoid X receptor. *Mol Endocrinol* 2003; **17**: 259–72.
5 Narisawa T, Magadia NE, Weisburger JH, Wynder EL. Promoting effect of bile acids on colon carcinogenesis after intrarectal instillation of N-methyl-N'-nitro-N-nitrosoguanidine in rats. *J Natl Cancer Inst* 1974; **53**: 1093–7.
6 Reddy BS, Watanabe K, Weisburger JH, Wynder EL. Promoting effect of bile acids in colon carcinogenesis in germ-free and conventional F344 rats. *Cancer Res* 1977; **37**: 3238–42.
7 Hirano F, Tanada H, Makino Y *et al.* Induction of the transcription factor AP-1 in cultured human colon adenocarcinoma cells following exposure to bile acids. *Carcinogenesis* 1996; **17**: 427–33.
8 Palmer DG, Paraskeva C, Williams AC. Modulation of p53 expression in cultured colonic adenoma cell lines by the naturally occurring lumenal factors butyrate and deoxycholate. *Int J Cancer* 1997; **73**: 702–6.
9 Matheson H, Branting C, Rafter I, Okret S, Rafter J. Increased c-fos mRNA and binding to the AP-1 recognition sequence accompanies the proliferative response to deoxycholate of HT29 cells. *Carcinogenesis* 1996; **17**: 421–6.
10 Glinghammar B, Holmberg K, Rafter J. Effects of colonic lumenal components on AP-1-dependent gene transcription in cultured human colon carcinoma cells. *Carcinogenesis* 1999; **20**: 969–76.
11 Halvorsen B, Staff AC, Ligaarden S, Prydz K, Kolset SO. Lithocholic acid and sulphated lithocholic acid differ in the ability to promote matrix metalloproteinase secretion in the human colon cancer cell line CaCo-2. *Biochem J* 2000; **349**: 189–93.
12 Glinghammar B, Rafter J. Colonic luminal contents induce cyclooxygenase 2 transcription in human colon carcinoma cells. *Gastroenterology* 2001; **120**: 401–10.
13 Qiao L, Studer E, Leach K *et al.* Deoxycholic acid (DCA) causes ligand-independent activation of epidermal growth factor receptor (EGFR) and FAS receptor in primary hepatocytes: inhibition of EGFR/mitogen-activated protein kinase-signaling module enhances DCA-induced apoptosis. *Mol Biol Cell* 2001; **12**: 2629–45.
14 Yoon JH, Higuchi H, Werneburg NW, Kaufmann SH, Gores GJ. Bile acids induce cyclooxygenase-2 expression via the epidermal growth factor receptor in a human cholangiocarcinoma cell line. *Gastroenterology* 2002; **122**: 985–93.
15 Stetler-Stevenson WG, Aznavoorian S, Liotta LA. Tumor cell interactions with the extracellular matrix during invasion and metastasis. *Annu Rev Cell Biol* 1993; **9**: 541–73.
16 Oka H, Shiozaki H, Kobayashi K *et al.* Expression of E-cadherin cell adhesion molecules in human breast cancer tissues and its relationship to metastasis. *Cancer Res* 1993; **53**: 1696–701.
17 Llorens A, Rodrigo I, Lopez-Barcons L *et al.* Down-regulation of E-cadherin in mouse skin carcinoma cells enhances a migratory and invasive phenotype linked to matrix metalloproteinase-9 gelatinase expression. *Laboratory Invest* 1998; **78**: 1131–42.
18 Luo J, Lubaroff DM, Hendrix MJ. Suppression of prostate cancer invasive potential and matrix metalloproteinase activity by E-cadherin transfection. *Cancer Res* 1999; **59**: 3552–6.
19 Pai R, Tarnawski AS, Tran T. Deoxycholic acid activates beta-catenin signaling pathway and increases colon cell cancer growth and invasiveness. *Mol Biol Cell* 2004; **15**: 2156–63.
20 Cano A, Perez-Moreno MA, Rodrigo I *et al.* The transcription factor snail controls epithelial-mesenchymal transitions by repressing E-cadherin expression. *Nat Cell Biol* 2000; **2**: 76–83.
21 Fujita N, Jaye DL, Kajita M, Geigerman C, Moreno CS, Wade PA. MTA3, a Mi-2/NuRD complex subunit, regulates an invasive growth pathway in breast cancer. *Cell* 2003; **113**: 207–19.
22 Barbera MJ, Puig I, Dominguez D *et al.* Regulation of Snail transcription during epithelial to mesenchymal transition of tumor cells. *Oncogene* 2004; **23**: 7345–54.
23 Pfeifer AM, Cole KE, Smoot DT *et al.* Simian virus 40 large tumor antigen-immortalized normal human liver epithelial cells express hepatocyte characteristics and metabolize chemical carcinogens. *Proc Natl Acad Sci USA* 1993; **90**: 5123–7.
24 Laffitte BA, Kast HR, Nguyen CM, Zavacki AM, Moore DD, Edwards PA. Identification of the DNA binding specificity and potential target genes for the farnesoid X-activated receptor. *J Biol Chem* 2000; **275**: 10638–47.
25 Song CS, Echchgadda I, Baek BS *et al.* Dehydroepiandrosterone sulfotransferase gene induction by bile acid activated farnesoid X receptor. *J Biol Chem* 2001; **276**: 42549–56.
26 Kast HR, Goodwin B, Tarr PT *et al.* Regulation of multidrug resistance-associated protein 2 (ABCC2) by the nuclear receptors pregnane X receptor, farnesoid X-activated receptor, and constitutive androstane receptor. *J Biol Chem* 2002; **277**: 2908–15.

27 Ohtsuka H, Abe T, Onogawa T *et al.* Farnesoid X receptor, hepatocyte nuclear factors 1alpha and 3beta are essential for transcriptional activation of the liver-specific organic anion transporter-2 gene. *J Gastroenterol* 2006; **41**: 369–77.
28 Edwards PA, Kast HR, Anisfeld AM. BAREing it all: the adoption of LXR and FXR and their roles in lipid homeostasis. *J Lipid Res* 2002; **43**: 2–12.
29 Hirano Y, Hirano F, Fujii H, Makino I. Fibrates suppress chenodeoxycholic acid-induced RANTES expression through inhibition of NF-kappaB activation. *Eur J Pharmacol* 2002; **448**: 19–26.
30 Suske G. The Sp-family of transcription factors. *Gene* 1999; **238**: 291–300.
31 Kollmar R, Sukow KA, Sponagle SK, Farnham PJ. Start site selection at the TATA-less carbamoyl-phosphate synthase (glutamine-hydrolyzing)/aspartate carbamoyltransferase/dihydroorotase promoter. *J Biol Chem* 1994; **269**: 2252–7.
32 Weis L, Reinberg D. Accurate positioning of RNA polymerase II on a natural TATA-less promoter is independent of TATA-binding-protein-associated factors and initiator-binding proteins. *Mol Cell Biol* 1997; **17**: 2973–84.
33 Wright KL, Vilen BJ, Itoh-Lindstrom Y *et al.* CCAAT box binding protein NF-Y facilitates *in vivo* recruitment of upstream DNA binding transcription factors. *EMBO J* 1994; **13**: 4042–53.
34 Bennett MK, Osborne TF. Nutrient regulation of gene expression by the sterol regulatory element binding proteins increased recruitment of gene-specific coregulatory factors and selective hyperacetylation of histone H3 *in vivo*. *Proc Natl Acad Sci USA* 2000; **97**: 6340–4.
35 Wu Z, Chiang JY. Transcriptional regulation of human oxysterol 7 alpha-hydroxylase gene (CYP7B1) by Sp1. *Gene* 2001; **272**: 191–7.
36 Husmann M, Dragneva Y, Romahn E, Jehnichen P. Nuclear receptors modulate the interaction of Sp1 and GC-rich DNA via ternary complex formation. *Biochem J* 2000; **352** (Pt 3): 763–72.
37 Shimada J, Suzuki Y, Kim SJ, Wang PC, Matsumura M, Kojima S. Transactivation via RAR/RXR–Sp1 interaction characterization of binding between Sp1 and GC box motif. *Mol Endocrinol* 2001; **15**: 1677–92.
38 Sinha S, Maity SN, Seldin MF, de Crombrugghe B. Chromosomal assignment and tissue expression of CBF-C/NFY-C, the third subunit of the mammalian CCAAT-binding factor. *Genomics* 1996; **37**: 260–3.
39 Kim IS, Sinha S, de Crombrugghe B, Maity SN. Determination of functional domains in the C subunit of the CCAAT-binding factor (CBF) necessary for formation of a CBF-DNA complex: CBF-B interacts simultaneously with both the CBF-A and CBF-C subunits to form a heterotrimeric CBF molecule. *Mol Cell Biol* 1996; **16**: 4003–13.
40 Liberati C, Ronchi A, Lievens P, Ottolenghi S, Mantovani R. NF-Y organizes the gamma-globin CCAAT boxes region. *J Biol Chem* 1998; **273**: 16880–9.
41 Wright KL, Moore TL, Vilen BJ, Brown AM, Ting JP. Major histocompatibility complex class II-associated invariant chain gene expression is up-regulated by cooperative interactions of Sp1 and NF-Y. *J Biol Chem* 1995; **270**: 20978–86.
42 Liang F, Schaufele F, Gardner DG. Functional interaction of NF-Y and Sp1 is required for type a natriuretic peptide receptor gene transcription. *J Biol Chem* 2001; **276**: 1516–22.
43 Gumbiner B, Stevenson B, Grimaldi A. The role of the cell adhesion molecule uvomorulin in the formation and maintenance of the epithelial junctional complex. *J Cell Biol* 1988; **107**: 1575–87.
44 Endo K, Ueda T, Ueyama J, Ohta T, Terada T. Immunoreactive E-cadherin, alpha-catenin, beta-catenin, and gamma-catenin proteins in hepatocellular carcinoma: relationships with tumor grade, clinicopathologic parameters, and patients' survival. *Hum Pathol* 2000; **31**: 558–65.
45 Batlle E, Sancho E, Franci C *et al.* The transcription factor snail is a repressor of E-cadherin gene expression in epithelial tumour cells. *Nat Cell Biol* 2000; **2**: 84–9.
46 Jiao W, Miyazaki K, Kitajima Y. Inverse correlation between E-cadherin and Snail expression in hepatocellular carcinoma cell lines *in vitro* and *in vivo*. *Br J Cancer* 2002; **86**: 98–101.
47 Sugimachi K, Tanaka S, Kameyama T *et al.* Transcriptional repressor snail and progression of human hepatocellular carcinoma. *Clin Cancer Res* 2003; **9**: 2657–64.
48 Poser I, Dominguez D, de Herreros AG, Varnai A, Buettner R, Bosserhoff AK. Loss of E-cadherin expression in melanoma cells involves up-regulation of the transcriptional repressor Snail. *J Biol Chem* 2001; **276**: 24661–6.

Supporting Information

Additional Supporting Information may be found in the online version of this article:

Table S1. Up- or down-regulated genes in THLE-3, Hep3B and HuCCT-1 cells.

Please note: Blackwell Publishing are not responsible for the content or functionality of any supporting materials supplied by the authors. Any queries (other than missing material) should be directed to the corresponding author for the article.

doi: 10.1111/j.1349-7006.2008.00898.x

European Journal of Endocrinology (2009) 160 459–463 ISSN 0804-4643

CLINICAL STUDY

Physiologic variance of corticotropin affects diagnosis in adrenal vein sampling

Masayuki Tanemoto, Takehiro Suzuki, Michiaki Abe, Takaaki Abe and Sadayoshi Ito

Division of Nephrology, Hypertension & Endocrinology, Department of Medicine, Graduate School of Medicine, Tohoku University, 1-1 Seiryo-cho, Aoba-ku, Sendai, Miyagi 980-8574, Japan

(Correspondence should be addressed to M Tanemoto; Email: mtanemoto-tky@umin.ac.jp)

Abstract

Objective: Differentiating unilateral form from bilateral is a critical diagnostic step in primary aldosteronism (PA), for which adrenal vein sampling (AVS) is accepted to be the most reliable. However, variance of corticotropin could affect the diagnosis in AVS.

Design and methods: We conducted simultaneous bilateral AVS on ten biochemically diagnosed PA cases, and used the aldosterone-to-cortisol ratio (A/C) of the samples for the diagnosis. The diagnosis by AVS after a low-dose (0.1 μg) ACTH stimulation, which can provoke maximum-physiologic corticotropic response, was compared with those before the stimulation and after the standard-dose (250 μg) ACTH stimulation.

Results: In half of the cases, the low-dose pre-stimulation affected the diagnosis. In four out of ten cases, the side-to-side ratios of A/C were changed in the basal/low-dose/standard-dose AVS as 6.62/2.46/0.63, 2.13/0.41/0.14, 1.88/2.38/2.40, and 1.96/2.27/1.90 respectively. In three out of ten cases, the adrenal vein to the matching inferior vena cava ratio of A/C was also changed across 1, the cut-off to indicate suppression of aldosterone secretion. Additionally, the confirmation of successful sampling was difficult in five out of ten and two out of ten cases of the basal and low-dose AVS respectively, whereas it was easy in all the cases of the standard-dose AVS.

Conclusions: The diagnosis in the basal AVS could be affected by the physiologic fluctuation of ACTH at relatively high prevalence. The basal AVS would be unreliable to differentiate two forms of PA.

European Journal of Endocrinology **160** 459–463

Introduction

Primary aldosteronism (PA) is recognized as a common cause of secondary hypertension, and is generally caused by either aldosterone-producing adenoma (commonly unilateral) or idiopathic hyperaldosteronism (commonly bilateral) (1–3). Differentiation of unilateral form from bilateral is a critical step in the diagnosis of PA, because the unilateral form is potentially curable by unilateral adrenalectomy and the bilateral form is generally treated with the administration of mineralocorticoid receptor antagonists.

Adrenal vein sampling (AVS) is the widely accepted way for differentiation, but the methodology used for AVS is different among different centers (3). Independent of the methodological difference, the following points are critical to perform adrenalectomy: i) confirmation of successful sampling and ii) certainty of the laterality of aldosterone hypersecretion. Adrenocortical hormones are under the effect of ACTH, and AVS without sufficient pre-stimulation could be affected by its fluctuation (4–6). Therefore, some investigators advocated pre-stimulation with synthetic corticotropin to ensure active adrenal secretion at the time of AVS (7–10). However, others expressed concern that the pre-stimulation could abolish the laterality of aldosterone secretion (11); the dose of synthetic corticotropin generally used for the pre-stimulation is extra-physiologically high (12, 13), and the exaggerated corticotropic response by it could conceal the laterality.

In this study, we performed AVS in three different conditions: before any artificial stimulation, after stimulation by a low-dose (0.1 μg) cosyntropin, which can provoke maximum-physiologic corticotropic response, and after stimulation by the standard-dose (250 μg) cosyntropin. We found that confirmation of successful sampling is difficult without sufficient pre-stimulation and that physiologically attainable corticotropin could affect the diagnosis in the AVS.

Subjects and methods

Subjects

The hypertensive patients with plasma renin activity (PRA; normal range: 0.2–2.7 ng/ml per h) <1.0 ng/ml per h and plasma aldosterone concentration (PAC;

DOI: 10.1530/EJE-08-0840
Online version via www.eje-online.org

normal range: 3.6–24 ng/dl) >12 ng/dl with the PAC-to-PRA ratio (PAC/PRA) >40 were further evaluated (14, 15). After the withdrawal of β-blockers and diuretics for at least 4 weeks, a captopril test was performed: PRA and PAC were measured at 60 or 90 min after an oral administration of 50 mg of captopril, and PAC/PRA was calculated (15). The patients with PAC/PRA >30 in the captopril test were given the biochemical diagnosis of PA (3). We enrolled ten of these cases in the study. The study protocol was approved by the ethics committee of our hospital, and informed consent was obtained from all the patients.

Simultaneous bilateral AVS

Catheterization of both femoral veins was performed in all the cases in the early afternoon (1300–1400 h). Blood samples of AVS for the measurement of PAC and plasma cortisol concentration were simultaneously obtained from both the AV and the infrarenal inferior vena cava (IVC; basal AVS). A low-dose cosyntropin (0.1 μg) was administered as an i.v. bolus, and the sampling was repeated 15 min later (low-dose AVS). After the low-dose AVS, the standard-dose cosyntropin (250 μg) was administered and the sampling was repeated 15 min later (standard-dose AVS). The patients were kept supine throughout the AVS procedure.

Chemical and hormonal assays

The serum creatinine concentration (sCr) and PRA were enzymatically measured. Plasma cortisol concentration was measured with a commercially available kit (Fluorescence Polarization Immunoassay, TDX/TDXFLX Cortisol; Abbott Japan Co. Ltd). The intra-assay coefficients of variation were 7.54–7.56, 2.94–3.20, and 1.98–2.30% for its low, medium, and high levels respectively. PAC was measured using commercial laboratory test services (Mitsubishi Chemical Medience, Tokyo, Japan). The reported intra-assay coefficients of variation were 8.3, 3.9, and 1.8% for PAC of 10.3, 33.6, and 73.2 ng/dl respectively.

Diagnosis in AVS

We used the PAC-to-plasma cortisol concentration ratio (A/C) of AVS samples for the diagnosis in AVS. The ratio of A/C in one AV to the other (the side-to-side ratio) was used to judge the laterality of aldosterone secretion; the ratios >4 and >2 were taken as conservative and aggressive cut-offs respectively (3, 7–9, 16). The AV-to-IVC ratio (AV/IVC) of A/C<1 was taken as the suppression of aldosterone secretion for the side (7, 8, 10).

Results

Baseline characteristics

The baseline characteristics of the patients are summarized in Table 1. Except for one case who had an sCr of 106.1 μmol/l, all the other cases had preserved renal function (sCr ≤88.4 μmol/l, normal range: 35.4–88.4 μmol/l). Half of the cases (5/10) had hypokalemia (serum potassium concentration ≤3.4 mmol/l, normal range: 3.5–4.8 mmol/l), and four out of five of them had PAC >24 ng/dl. All the cases who did not have hypokalemia had PAC <24 ng/dl. The plasma corticotropin was less than its upper normal limit (normal range: 9–52 pg/ml).

Aldosterone and cortisol concentration in AVS

The results of AVS are shown in Table 2. The low-dose pre-stimulation increased PAC and plasma cortisol concentration in the AV samples except for one sample, and the standard-dose pre-stimulation increased them in all the AV samples. The pre-stimulation increased the AV/IVC of plasma cortisol concentration in all the AV samples, and the ratios were >1.6, >1.9, and >19 in the basal, low-dose, and standard-dose AVS respectively.

Laterality of aldosterone secretion

The side-to-side ratio of A/C is summarized in Table 3. Seven cases had the ratio in the basal AVS higher than the conservative cut-off (>4). In six of them, the ratio remained >4 in both the low- and standard-dose AVS. In the other case with the ratio of 6.62 (case 1), however, the ratio decreased to 2.46 (lower than the conservative cut-off, but higher than the aggressive cut-off) in the low-dose AVS. It decreased further to 0.63 and the laterality was changed in the standard-dose AVS, but its reciprocal ratio was lower than the aggressive cut-off (<2).

Three cases had the ratio in the basal AVS lower than the conservative cut-off (<4). In one case with the ratio higher than the aggressive cut-off (2.13, case 2), the laterality was changed in the low-dose AVS and the reciprocal ratio was 2.47 (lower than the conservative

Table 1 Baseline characteristics of patients.

Number (% female)	10 (30)
Age (years)	55±13 (34–71)
sCr (μmol/l)	73.4±15.6 (35.4–106.1)
sK^+ (mmol/l)	3.4±0.6 (2.3–4.0)
ACTH (pg/ml)	16.1±7.2 (6.2–32.7)
PRA (ng/ml per hour)	0.2±0.1 (0.1–0.4)
PAC (ng/dl)	33.0±21.7 (13.5–66.8)
PAC/PRA	258±220 (55.5–668)

Values are expressed as mean±s.d. with their distribution given in parentheses, where appropriate. sCr, serum creatinine concentration; sK^+; serum potassium concentration; PRA, plasma renin activity; PAC, plasma aldosterone concentration.

Table 2 Results of adrenal vein sampling (AVS).

Case		Basal		Low dose		Standard dose	
		PAC	Cortisol	PAC	Cortisol	PAC	Cortisol
1	R/L	1558/177	22.1/16.6	1939/869	128/141	3643/3559	925/565
	IVC	9.7	3.7	16.6	7.1	25.9	22.0
2	R/L	401/136	18.4/13.2	317/508	171/111	648/7680	520/880
	IVC	11.8	2.8	11.9	5.5	21.6	13.9
3	R/L	61.7/20.3	84.0/54.2	594/221	341/288	2518/896	1159/785
	IVC	6.2	15.4	4.2	15.4	10.6	23.6
4	R/L	34.5/53.8	16.8/13.9	223/244	115/53	1310/2623	621/531
	IVC	9.3	6.9	11.2	8.2	16.4	18.9
5	R/L	498/17.5	18.2/17.1	2026/216	244/174	4432/592	443/492
	IVC	10.6	7.2	17.9	15.3	27	23.7
6	R/L	318/8.7	26/27	386/8.5	28.4/26	7667/447	1051/735
	IVC	7.5	15.7	8.1	13.5	20	25.5
7	R/L	2467/52.7	19.2/15.6	2269/125	20.9/304	10853/458	688/801
	IVC	61.3	5.5	72	10.1	80.0	18.2
8	R/L	563/17.7	17.9/17.1	1543/74.8	359/109	20006/373	521/438
	IVC	13.7	10.5	23.0	14.7	46.0	23.0
9	R/L	942/44.4	33.3/40.4	1964/177	404/424	3531/352	555/823
	IVC	42.9	8.9	45.5	15.0	60.5	26.2
10	R/L	34.9/2904	20.7/17.7	130/4001	275/362	475/8451	1354/1071
	IVC	39.6	2.6	51.3	7.6	79.5	25.5

PAC, plasma aldosterone concentration (ng/dl); cortisol, plasma cortisol concentration (μg/dl); R, right adrenal vein; L, left adrenal vein; IVC, inferior vena cava.

cut-off, but higher than the aggressive cut-off). The reciprocal ratio increased further to 7.01, higher than the conservative cut-off, in the standard-dose AVS. The other two cases (cases 3 and 4) had the ratio in the basal AVS lower than the aggressive cut-off (<2). In these cases, the laterality was not changed, but the ratio increased to >2 in the low-dose AVS; the ratios in the basal/low-dose/standard-dose AVS were 1.88/2.38/2.40 and 1.96/2.27/1.90 respectively.

Suppression of aldosterone secretion

The suppression of aldosterone secretion, which was indicated by the AV/IVC of A/C <1, was also changed by the pre-stimulation in three cases (Table 4). Two cases (cases 3 and 5), which had the ratio of one side <1 in the basal AVS, had the ratio of the both sides >1 in both the low- and standard-dose AVS. Conversely, one case (case 2), which had the ratio of the both sides >1 in the basal AVS, had the ratio of one side <1 in both the low- and standard-dose AVS.

Table 3 The side-to-side ratio of aldosterone-to-cortisol ratio.

Case		Basal	Low dose	Standard dose
1	R/L (L/R)	6.62 (0.15)	2.46 (0.41)	0.63 (1.60)
2	R/L (L/R)	2.13 (0.47)	0.40 (2.47)	0.14 (7.01)
3	R/L (L/R)	1.96 (0.51)	2.27 (0.44)	1.90 (0.53)
4	R/L (L/R)	0.55 (1.88)	0.42 (2.38)	0.42 (2.40)
5	R/L (L/R)	26.8 (0.04)	6.68 (0.15)	8.32 (0.12)
6	R/L (L/R)	37.9 (0.03)	41.5 (0.02)	12.0 (0.08)
7	R/L (L/R)	38.1 (0.03)	264 (0.00)	27.6 (0.04)
8	R/L (L/R)	30.3 (0.03)	6.25 (0.16)	45.1 (0.02)
9	R/L (L/R)	25.7 (0.04)	11.7 (0.09)	14.9 (0.07)
10	R/L (L/R)	0.01 (97.7)	0.04 (23.4)	0.04 (22.5)

A/C, plasma aldosterone concentration (ng/dl)/plasma cortisol concentration (μg/dl); R, right adrenal vein; L, left adrenal vein.

Discussion

In this study, we showed that the diagnosis in the basal AVS could be affected by the physiologic fluctuation of ACTH at the time of AVS. The fluctuation could affect either the laterality or the suppression of aldosterone secretion at relatively high prevalence. In addition, we also showed that confirmation of successful sampling is difficult without sufficient pre-stimulation.

In the basal AVS, six cases had PAC of IVC <12 ng/dl, although we selected cases of the baseline PAC >12 ng/dl. The usage of calcium channel blockers, which can suppress aldosterone secretion, could have decreased the PAC of IVC in the basal AVS, because we used them to control blood pressure during AVS (17, 18). It is also possible that the difference between the PAC of IVC in the basal AVS and the baseline PAC reflected the physiologic fluctuation of PAC, because we performed AVS in the early afternoon (5). Performance of AVS in the early afternoon is the main limitation of this study. The difference between the basal and low-dose AVS might have been decreased if AVS were performed in the morning when ACTH is generally higher than in the afternoon.

For the pre-stimulation, we used cosyntropin, a synthetic corticotropin, which has corticotropic potency as the natural corticotropin (19). A bolus injection of 0.1 μg cosyntropin is expected to elevate its plasma concentration to ~200 pg/ml (12). The insulin

Table 4 The adrenal vein/inferior vena cava of aldosterone-to-cortisol ratio.

Case		Basal	Low dose	Standard dose
1	R/L	27.0/4.07	6.54/2.66	3.39/5.42
2	R/L	5.26/2.47	0.85/2.10	0.85/5.63
3	R/L	1.83/0.93	6.28/2.81	4.84/2.54
4	R/L	1.52/2.87	1.42/3.37	2.44/5.70
5	R/L	18.5/0.69	7.08/1.06	8.79/1.06
6	R/L	25.6/0.68	22.7/0.55	9.29/0.77
7	R/L	11.5/0.30	15.2/0.06	3.60/0.13
8	R/L	24.1/0.79	2.75/0.44	19.2/0.43
9	R/L	5.87/0.23	1.60/0.14	2.79/0.19
10	R/L	0.11/10.8	0.07/1.63	0.11/2.53

AV, adrenal vein; IVC, inferior vena cava; A/C plasma aldosterone concentration (ng/dl)/plasma cortisol concentration (μg/dl); R, right adrenal vein; L, left adrenal vein.

hypoglycemic test, an acknowledged test to provoke maximum physiologic response of the pituitary–adrenal axis, can elevate plasma ACTH concentration to 100–300 pg/ml (20). Therefore, the low-dose pre-stimulation is thought to induce the maximum-physiologic but not supra-physiologic corticotropic response. Supporting this notion, the plasma cortisol concentration in the low-dose AVS was lower than its matching concentration in the standard-dose AVS.

After the low-dose AVS, we conducted the standard-dose AVS consecutively. The preceding stimulation could have modified the adrenal response to the following stimulation. However, the preceding low-dose AVS is not thought to have significantly modified the following standard-dose AVS in the present cases, because the adrenal response in the standard-dose AVS was several times higher than that in the low-dose AVS. The preserved adrenal response after the preceding 0.5 μg cosyntropin stimulation is also reported; the response to 250 μg stimulation after the preceding 0.5 μg stimulation is more than half of its maximum response (13).

The AV/IVC ratio of plasma cortisol concentration is widely used as an index for successful sampling. Its values from >1.1 to >5 are used for the judgment with lower values for the basal AVS than the pre-stimulated AVS (7, 11, 21, 22); the ratio >3 and >5 can be considered as conservative cut-offs for the former and the latter respectively. Using these conservative cut-offs, 9 out of 20 of the basal AVS samples and 3 out of 20 of the low-dose AVS samples are taken as unsuccessful, whereas all the standard-dose AVS samples are taken as successful. Consequently, only in half of the present cases, all three sets of AVS were taken successful by the conservative cut-offs. However, we verified the position of the catheter tip in each sampling by gentle injection of a small amount of contrast medium, and confirmed accomplishment of three sets of AVS at the same position in each case. Therefore, the result of basal and low-dose AVS samples being taken as unsuccessful by the conservative cut-offs indicates difficulty in confirming successful sampling without sufficient pre-stimulation. Difficulty in confirming successful sampling without pre-stimulation is also reported; nearly half of the basal AVS samples that the radiologist considered successful do not have the ratio >3 (21).

Unilateral form of aldosterone secretion is generally indicated in two ways: (i) laterality of secretion, which is judged by the side-to-side ratio of A/C either >4–5 (3, 7–9) or >2 (16) and (ii) suppression of secretion from the other side, which is judged by the AV/IVC of A/C <1 (7, 8, 10). The low-dose pre-stimulation affected either the laterality or the suppression in half of the present cases. In a subset of the cases in whom all three sets of AVS were taken as successful by the conservative cut-offs, the low-dose pre-stimulation also affected either the laterality or the suppression in two out of five cases. These results indicate that the diagnosis in the basal AVS is unreliable; the physiologic fluctuation of ACTH could change the diagnosis in the basal AVS (4). Supporting this notion, we experienced wide case-dependent difference of the basal ACTH stimulation (6).

Slight difference of each ratio is practically indistinguishable due to the variation of the intra-assay coefficients for PAC and plasma cortisol concentration, and the diagnosis in cases 3, 4, and 5 could be taken the same in all three types of AVS. However, the diagnosis in cases 1 and 2 could not be taken the same. The pre-stimulation amply changed the side-to-side ratio of A/C across the cut-offs, although both cases could be taken as bilateral lack of suppression independent of the pre-stimulation. These controversial cases did not undergo adrenalectomy, because they could be bilateral forms. Without histological confirmation, we could not determine which set of AVS was accurate, but we think that the diagnostic AVS should be performed under constant conditions such as after sufficient ACTH stimulation. Difficulty in confirmation of successful sampling without sufficient pre-stimulation also supports the necessity of ACTH stimulation in the diagnostic AVS.

In summary, the results of this study indicate that the physiologic fluctuation of ACTH can affect the diagnosis in the basal AVS. Although the enrollment was small, the high prevalence with diagnostic change by the physiologically attainable corticotropin indicates that the diagnosis in the basal AVS is unreliable in not a few cases. Difficulty in confirmation of successful sampling is another disadvantage of the basal AVS. Therefore, AVS with sufficient pre-stimulation, such as the standard-dose AVS, is preferable, especially when the basal AVS is difficult to be taken successful.

Declaration of interest

There is no conflict of interest that could be perceived as prejudicing the impartiality of the research reported.

Funding

This study was supported by the grants from the Ministry of Education, Culture, Sports, Science and Technology of Japan, and from the Salt Science Research Foundation (no. 0734 and 08C2).

References

1 Mattsson C & Young WF Jr. Primary aldosteronism: diagnostic and treatment strategies. *Nature Clinical Practice. Nephrology* 2006 **2** 198–208.

2 Schirpenbach C & Reincke M. Primary aldosteronism: current knowledge and controversies in Conn's syndrome. *Nature Clinical Practice. Endocrinology and Metabolism* 2007 **3** 220–227.

3 Funder JW, Carey RM, Fardella C, Gomez-Sanchez CE, Mantero F, Stowasser M, Young WF Jr & Montori VM. Case detection, diagnosis, and treatment of patients with primary aldosteronism: an endocrine society clinical practice guideline. *Journal of Clinical Endocrinology and Metabolism* 2008 **93** 3266–3281.

4 Sragy HM, Vieweg WV, Pincus S & Veldhuis JD. Increased disorderliness and amplified basal and pulsatile aldosterone secretion in patients with primary aldosteronism. *Journal of Clinical Endocrinology and Metabolism* 1995 **80** 28–33.

5 Kem DC, Weinberger MH, Gomez-Sanchez C, Kramer NJ, Lerman R, Furuyama S & Nugent CA. Circadian rhythm of plasma aldosterone concentration in patients with primary aldosteronism. *Journal of Clinical Investigation* 1973 **52** 2272–2277.

6 Tanemoto M, Satoh F, Abe T & Ito S. To stimulate or not to stimulate: is adrenocorticotrophic hormone testing necessary, or not? – round 2 *Journal of Hypertension* 2007 **25** 1517–1518.

7 Magill SB, Raff H, Shaker JL, Brickner RC, Knechtges TE, Kehoe ME & Findling JW. Comparison of adrenal vein sampling and computed tomography in the differentiation of primary aldosteronism. *Journal of Clinical Endocrinology and Metabolism* 2001 **86** 1066–1071.

8 Phillips JL, Walther MM, Pezzullo JC, Rayford W, Choyke PL, Berman AA, Linehan WM, Doppman JL & Gill JR Jr. Predictive value of preoperative tests in discriminating bilateral adrenal hyperplasia from an aldosterone-producing adrenal adenoma. *Journal of Clinical Endocrinology and Metabolism* 2000 **85** 4526–4533.

9 Young WF, Stanson AW, Thompson GB, Grant CS, Farley DR & van Heerden JA. Role for adrenal venous sampling in primary aldosteronism. *Surgery* 2004 **136** 1227–1235.

10 Doppman JL & Gill JR Jr. Hyperaldosteronism: sampling the adrenal veins. *Radiology* 1996 **198** 309–312.

11 Rossi GP, Ganzaroli C, Miotto D, De Toni R, Palumbo G, Feltrin GP, Mantero F & Pessina AC. Dynamic testing with high-dose adrenocorticotrophic hormone does not improve lateralization of aldosterone oversecretion in primary aldosteronism patients. *Journal of Hypertension* 2006 **24** 371–379.

12 Mayenknecht J, Diederich S, Bahr V, Plockinger U & Oelkers W. Comparison of low and high dose corticotropin stimulation tests in patients with pituitary disease. *Journal of Clinical Endocrinology and Metabolism* 1998 **83** 1558–1562.

13 Arvat E, Di Vito L, Lanfranco F, Maccario M, Baffoni C, Rossetto R, Almaretti G, Camanni F & Ghigo E. Stimulatory effect of adrenocorticotropin on cortisol, aldosterone, and dehydroepiandrosterone secretion in normal humans: dose–response study. *Journal of Clinical Endocrinology and Metabolism* 2000 **85** 3141–3146.

14 Giacchetti G, Ronconi V, Lucarelli G, Boscaro M & Mantero F. Analysis of screening and confirmatory tests in the diagnosis of primary aldosteronism: need for a standardized protocol. *Journal of Hypertension* 2006 **24** 737–745.

15 Seiler L, Rump LC, Schulte-Monting J, Slawik M, Born K, Pavenstadt H, Beuschlein F & Reincke M. Diagnosis of primary aldosteronism: value of different screening parameters and influence of antihypertensive medication. *European Journal of Endocrinology* 2004 **150** 329–337.

16 Rossi GP, Sacchetto A, Chiesura-Corona M, De Toni R, Gallina M, Feltrin GP & Pessina AC. Identification of the etiology of primary aldosteronism with adrenal vein sampling in patients with equivocal computed tomography and magnetic resonance findings: results in 104 consecutive cases. *Journal of Clinical Endocrinology and Metabolism* 2001 **86** 1083–1090.

17 Nadler JL, Hsueh W & Horton R. Therapeutic effect of calcium channel blockade in primary aldosteronism. *Journal of Clinical Endocrinology and Metabolism* 1985 **60** 896–899.

18 Veglio F, Pinna G, Bisbocci D, Rabbia F, Piras D & Chiandussi L. Efficacy of nicardipine slow release (SR) on hypertension, potassium balance and plasma aldosterone in idiopathic aldosteronism. *Journal of Human Hypertension* 1990 **4** 579–582.

19 Landon J, James VH, Cryer RJ, Wynn V & Frankland AW. Adrenocorticotropic effects of a synthetic polypeptide-Beta 1-24-corticotropin – in man. *Journal of Clinical Endocrinology and Metabolism* 1964 **24** 1206–1213.

20 Oelkers W. The role of high- and low-dose corticotropin tests in the diagnosis of secondary adrenal insufficiency. *European Journal of Endocrinology* 1998 **139** 567–570.

21 Harvey A, Kline G & Pasieka JL. Adrenal venous sampling in primary hyperaldosteronism: comparison of radiographic with biochemical success and the clinical decision-making with 'less than ideal' testing. *Surgery* 2006 **140** 847–853.

22 Espiner EA, Ross DG, Yandle TG, Richards AM & Hunt PJ. Predicting surgically remedial primary aldosteronism: role of adrenal scanning, posture testing, and adrenal vein sampling. *Journal of Clinical Endocrinology and Metabolism* 2003 **88** 3637–3644.

Received 27 November 2008
Accepted 28 November 2008

Profiling SLCO and SLC22 genes in the NCI-60 cancer cell lines to identify drug uptake transporters

Mitsunori Okabe,[1] Gergely Szakács,[1,3] Mark A. Reimers,[2,4] Toshihiro Suzuki,[1,5] Matthew D. Hall,[1] Takaaki Abe,[6] John N. Weinstein,[2] and Michael M. Gottesman[1]

Laboratories of [1]Cell Biology and [2]Molecular Pharmacology, Center for Cancer Research, National Cancer Institute, NIH, Bethesda, Maryland; [3]Institute of Enzymology, Biological Research Center, Hungarian Academy of Sciences, Budapest, Hungary; [4]Department of Biostatistics, Virginia Commonwealth University, Richmond, Virginia; [5]Department of Analytical Biochemistry, Meiji Pharmaceutical University, Tokyo, Japan; and [6]Division of Nephrology, Endocrinology, and Vascular Medicine, Department of Medicine, Tohoku University Graduate School of Medicine, Sendai, Japan

Abstract

Molecular and pharmacologic profiling of the NCI-60 cell panel offers the possibility of identifying pathways involved in drug resistance or sensitivity. Of these, decreased uptake of anticancer drugs mediated by efflux transporters represents one of the best studied mechanisms. Previous studies have also shown that uptake transporters can influence cytotoxicity by altering the cellular uptake of anticancer drugs. Using quantitative real-time PCR, we measured the mRNA expression of two solute carrier (SLC) families, the organic cation/zwitterion transporters (SLC22 family) and the organic anion transporters (SLCO family), totaling 23 genes in normal tissues and the NCI-60 cell panel. By correlating the mRNA expression pattern of the SLCO and SLC22 family member gene products with the growth-inhibitory profiles of 1,429 anticancer drugs and drug candidate compounds tested on the NCI-60 cell lines, we identified SLC proteins that are likely to play a dominant role in drug sensitivity. To substantiate some of the SLC-drug pairs for which the SLC member was predicted to be sensitizing, follow-up experiments were performed using engineered and characterized cell lines overexpressing SLC22A4 (OCTN1). As predicted by the statistical correlations, expression of SLC22A4 resulted in increased cellular uptake and heightened sensitivity to mitoxantrone and doxorubicin. Our results indicate that the gene expression database can be used to identify SLCO and SLC22 family members that confer sensitivity to cancer cells. [Mol Cancer Ther 2008;7(9):3081–91]

Introduction

One of the major mechanisms of adaptive cellular anticancer drug resistance [multidrug resistance (MDR)] is diminished cellular accumulation conferred by a combination of decreased transporter-mediated drug uptake and increased energy-dependent efflux of drugs (1). This occurs in concert with a variety of metabolic changes in cells that affect the ability of cytotoxic drugs to kill cells, including alterations in the cell cycle, increased repair of DNA damage, reduced apoptosis, and altered metabolism of drugs. Of these mechanisms, the one most commonly encountered in the laboratory is the increased efflux of a broad range of cytotoxic drugs mediated by ATP binding cassette (ABC) transporters (2). P-glycoprotein, encoded by *ABCB1* (also known as *MDR1*), stands out among ABC transporters by conferring the strongest resistance to a wide variety of drugs and has been shown to be implicated in clinical drug resistance (3). In addition to P-glycoprotein, 11 of 48 known human ABC transporters have been shown to play some role in the drug resistance of cancer cells *in vivo* and/or *in vitro* (4).

Recently, we have used a bioinformatic approach to identify ABC transporter substrates. We profiled mRNA expression of all 48 ABC transporters in 60 diverse cancer cell lines (the NCI-60) used by the National Cancer Institute to screen for anticancer activity of >100,000 compounds submitted for testing. In our previous study, by correlating the expression profiles with the growth-inhibitory profiles of a subset of 1,429 compounds (incorporating anticancer drugs and drug candidates) tested against the cells, we successfully identified several cytotoxic substrates recognized by different ABC transporters (5).

As mentioned above, resistance can also result from reduced transporter-mediated drug uptake, and the net accumulation of an anticancer drug in a cell is probably influenced by the concurrent actions of uptake and efflux transporters. The solute carrier (SLC) gene series encodes a large family of passive transporters, ion-coupled transporters, and exchangers that rely on a concentration gradient across the membrane or cotransport/countertransport to facilitate substrate transport. In the physiologic setting, SLC transporters are responsible for the absorption and excretion of a wide variety of endogenous and exogenous compounds. The human organic anion

Received 3/7/08; revised 6/9/08; accepted 6/30/08.

Grant support: Intramural Research Program of the NIH, National Cancer Institute, and Japan Society for the Promotion of Science. G. Szakács is a Bolyai fellow and a special fellow of the Leukemia and Lymphoma Society.

The costs of publication of this article were defrayed in part by the payment of page charges. This article must therefore be hereby marked *advertisement* in accordance with 18 U.S.C. Section 1734 solely to indicate this fact.

Requests for reprints: Michael M. Gottesman, Laboratory of Cell Biology, Center for Cancer Research, National Cancer Institute, NIH, Bethesda, MD 20892. Phone: 301-496-1530; Fax: 301-402-0450; E-mail: mgottesman@nih.gov

doi:10.1158/1535-7163.MCT-08-0539

transporting peptide (OATP or SLC21) family is composed of 11 members that transport endogenous organic anions (e.g., bile salts and bilirubin) and xenobiotics. The organic cation (and carnitine) transporter (OCT, SLC22) family has members that are able to transport organic cations/zwitterions and anions (6–8). Within the SLC22 family, there are six main cation transporters; SLC22A1 (OCT1), SLC22A2 (OCT2), SLC22A3 (OCT3), SLC22A4 (OCTN1), SLC22A5 (OCTN2), and SLC2A16 (OCT6), three of which are known to transport the zwitterion carnitine (SLC22A4, SLC22A5, and SLC22A16; ref. 8).

Studies have proven that uptake transporters can indeed confer sensitivity to anticancer drugs (9–14). For example, methotrexate has been shown to be a substrate for organic anion-transporting polypeptide 1B3 (SLCO1B3, OATP1B3; ref. 9). (Note: In this report, we refer to individual proteins of the SLCO and SLC22 family by using series numbers for SLC genes and also the general protein nomenclature. See http://www.genenames.org/.) Similarly, studies have shown that the organic cation transporters SLC22A1 (OCT1), SLC22A2 (OCT2), and SLC22A3 (OCT3) mediate cell sensitivity to platinum drugs such as cisplatin, carboplatin, and oxaliplatin (12–15).

Huang et al. have exploited the NCI-60 database to correlate oligonucleotide array data with the potencies of 119 standard anticancer drugs and showed that SLC29A1 plays a role in the cellular uptake of the nucleoside analogues azacytidine and inosine-glycodialdehyde (16). In this study, we have measured the mRNA expression of two SLC families in normal human tissues and the NCI-60 cell line panel. Because reproducible, quantitative correlations between the expression and the sensitivity were required, we chose to measure transcript expression by quantitative real-time PCR to gain a perspective on the potential role of SLCO and SLC22 transporters in drug response. We show that positively correlated drug-gene pairs reveal SLC transporters conferring chemosensitivity to their respective drug substrates. In particular, the pharmacogenomic approach based on the correlation of expression and sensitivity data sets derived from the NCI-60 cell panel identifies SLC22A4 (OCTN1) as a candidate drug transporter. We generated a KB-3-1 cell line transfected with a plasmid expressing SLC22AA4, and our *in vitro* experiments confirm that SLC22A4 mediates the cellular uptake of mitoxantrone and doxorubicin, thereby conferring cellular sensitivity to these agents.

Materials and Methods

Chemicals

Tetraethylammonium chloride (TEA), mitoxantrone dihydrochloride, and doxorubicin hydrochloride were obtained from Sigma. NSC59729 and NSC251819 were obtained from the National Cancer Institute Developmental Therapeutics Program (DTP). Solutions of TEA (10 mmol/L), mitoxantrone (20 mmol/L), doxorubicin (20 mmol/L), NSC59729 (20 mmol/L), and NSC251819 (20 mmol/L) were prepared using the same buffer as employed in uptake assays (described below). Stock solutions were aliquoted and stored at -80°C. [ethyl 1-^{14}C]TEA bromide (55.0 mCi/mmol) and [^{3}H(G)]mitoxantrone (1.5 Ci/mmol) were from American Radiolabeled Chemicals, and (14) doxorubicin hydrochloride (55.0 mCi/mmol) was from Amersham. All other chemicals and reagents were of analytical grade.

Preparation of Total RNA

Total RNA from human normal tissues was obtained from Clontech. Total RNA from the 60 cancer cell lines was prepared and provided by DTP.[7] For consistency in RNA quality, DTP has adopted standard operating procedures that include the use of matched serum batches and harvesting the cells at a particular confluence (17). Nevertheless, the quality (purity and integrity) of the RNA samples was assessed using an Agilent 2100 Bioanalyzer. The RNA was quantitated using a spectrophotometer (Ultrospec 3100 pro; Amersham).

Real-time Quantitative Reverse Transcription-PCR

Expression levels of the SLCO and SLC22 family genes were measured by real-time quantitative reverse transcription-PCR (RT-PCR) using ABI PRISM 7900HT (Applied Biosystems). For information on specific oligonucleotide primers and TaqMan probes for each of the SLC members, see Supplementary Tables S4 and S5. Synthesis of cDNA from total RNA samples was carried out using TaqMan Reverse Transcription Reagents (Applied Biosystems) with 1 μg total RNA/50 μL reaction volume. The cDNA (0.5 μL reverse transcription sample) was amplified using TaqMan Universal PCR Master Mix Reagents (Applied Biosystems) in a total volume of 10 μL. The PCR mixture was preincubated at 50°C for 2 min, incubated at 95°C for 10 min, and amplified by 40 cycles at 95°C for 15 s and 60°C for 1 min. No-template (water) reaction mixtures were prepared as negative controls.

Data Processing

During the PCR amplification, fluorescence emission was measured and recorded in real time. Crossing point (CP) values were calculated using the ABI PRISM 7900HT software package. The raw results were expressed as number of cycles to reach the CP. If the desired product was not detected, the corresponding value was adjusted to CP indicating no expression. To assess the contribution of experimental error, cell lines were assessed in triplicate. The average pair-wise correlation of triplicate expression profiles was 0.90. One of the most important steps in the design of quantitative PCR experiments is the choice of adequate internal controls. A reliable standard gene is expected to show unchanged expression under all experimental conditions. We found that the expression levels of five housekeeping genes (glyceraldehyde-3-phosphate dehydrogenase, tyrosine 3-monooxygenase/tryptophan 5-monooxygenase activation protein, and ζ polypeptide, ubiquitin C, hypoxantine phosphoribosyltransferase 1, and β-actin) are highly variable across the 60 cell lines and 29 human tissues (data not shown; however,

[7] http://www.dtp.nci.nih.gov/branches/btb/ivclsp.html

see ref. 18). Hence, as in our previous study (5), they were not used as controls. Because the majority of the studied genes are not expected to be consistently changed across the cells, we chose to internally normalize the samples (genes in a cell) with respect to the mean expression of the characterized genes. Finally, the values were multiplied by -1 so that positive values indicate higher expression.

Drug Database

More than 100,000 chemical compounds have been tested in the NCI-60 screen by the DTP. For this study, we focused on a subset consisting of 1,429 compounds that have been tested at least four times on all or most cell lines in the NCI-60 and whose screening data met quality control criteria described elsewhere (19). This subset includes most of the drugs currently used clinically for cancer treatment along with many candidates that have reached clinical trials.[8]

Statistical Analysis of Real-time Quantitative RT-PCR

Basic descriptive statistics were done using the CIMminer tool (http://discover.nci.nih.gov) and the R statistical programming language (http://www.r-project.org). A two-dimensional agglomerative hierarchical cluster analysis, with average linkage algorithm and distance metric $1 - r$, where r is the Pearson's correlation coefficient, was done using CIMminer to group the 60 cell lines as well as SLCO and SLC22 family members based on their expression profiles. The resulting matrix of numbers was displayed in clustered image map form (20). To select drug candidates for detailed follow-up, we used both a simple Bonferroni procedure and the Benjamini-Hochberg False Discovery Rate procedure (21) to adjust for multiple testing of all 28 genes and all 1,429 compounds simultaneously.

Establishment of Stable Transfectants

A plasmid containing the full-length cDNA of human *SLC22A4* (reference sequence: NM_003059) was obtained from OriGene. The cDNA was amplified by PCR using specific primers (Lofstrand). The amplified PCR product was subcloned into expression vector pcDNA 3.1/V5-His-TOPO (Invitrogen). The inserted *SLC22A4* was sequenced by the National Cancer Institute DNA Sequencing Facility. Using Lipofectamine (Invitrogen), the expression construct was transfected into KB-3-1 cells. KB-3-1 cells transfected with mock vector (pcDNA3.1/V5-His-TOPO/*lacZ*) served as a control. Stable clones were selected with 0.8 mg/mL G418 sulfate. Among the G418-resistant clones, the stable transfectants expressing SLC22A4 (OCTN1) were characterized by real-time quantitative RT-PCR, Western blot analysis, immunocytochemical analysis, and by measuring the uptake of [^{14}C]TEA, a known substrate of SLC22A4 (OCTN1). The selected clones [SLC22A4 (OCTN1)/KB-3-1 and Mock/KB-3-1] were used for drug sensitivity and uptake assays.

Cell Culture

The culture medium for stable transfectants was DMEM supplemented with 10% fetal bovine serum (Life Technologies/Invitrogen), 100 units/mL penicillin G, 100 μg/mL streptomycin, 2 mmol/L L-glutamine, and 0.4 mg/mL G418. Cells were grown at 37°C in a humidified atmosphere with 5% CO_2 and 95% air.

Western Blot Analysis

Crude membrane fractions from the cells stably transfected with SLC22A4 (OCTN1) and mock-vector were collected using the Qproteome Cell Compartment Kit (Qiagen). The proteins (10 μg/lane) were separated on 4% to 12% gradient SDS-polyacrylamide gels and then blotted onto a PVDF membrane. The membrane was blocked with TBS-0.05% Tween 20 and 5% skimmed milk for 1 h at room temperature. After washing with TBS-0.05% Tween 20, the membrane was incubated with anti-V5-HRP antibody (Invitrogen) diluted 1:5,000 in TBS-0.05% Tween 20 overnight at room temperature. The membrane was then washed with TBS-0.05% Tween 20, and proteins were visualized using the SuperSignal West chemiluminescent substrate (Pierce).

Immunocytochemical Analysis

Cells were grown on chamber slides. Twenty-four hours after seeding, the cells were fixed (100% methanol for 5 min at room temperature), permeabilized (0.1% Triton X-100 for 3 min at room temperature), blocked (PBS/10% fetal bovine serum for 30 min at room temperature), and incubated with anti-V5-FITC antibody (Invitrogen) diluted 1:500 in PBS/10% fetal bovine serum for 2 h at room temperature. After a wash with PBS, Vectashield mounting medium (Vector) was added. Fluorescent cells were examined under a confocal laser scanning fluorescence microscope (LSM510; Carl Zeiss).

Drug Sensitivity Assay

Cells were seeded in 100 μL culture medium without G418 at a density of 3,000 per well in 96-well plates and incubated for 24 h. Medium containing serially diluted mitoxantrone, doxorubicin, NSC59729, or NSC251819 was added to give the indicated final concentrations in three replicated wells. Cells were then incubated for 72 h. The antiproliferative activities of drugs were evaluated using CCK-8 (Cell Counting Kit-8) following the manufacturer's instructions (Dojindo). Maximal cell survival (defined as 100%) represented wells without drug. Dose-response curves were plotted using GraphPad PRISM software.

Uptake Assay

Cells were seeded in the culture medium without G418 at a density of 2.0×10^5 per well in 24-well plates and incubated for 24 h. Before initiation of the assay, cells were washed with an uptake buffer containing 125 mmol/L NaCl, 20 mmol/L $NaHCO_3$, 3 mmol/L KCl, 1.8 mmol/L $CaCl_2$, 1 mmol/L KH_2PO_4, 1.2 mmol/L $MgSO_4$, 10 mmol/L D-glucose, and 10 mmol/L HEPES (pH 7.4) and preincubated in the same buffer for 5 min. The assay was initiated by replacing the uptake buffer with 0.1 mL of the same buffer containing radiolabeled drugs. For the time course of the uptake, cells were incubated with 3 μmol/L [^{3}H]mitoxantrone or [^{14}C]doxorubicin for the designated period in an incubator (5% CO_2, 95% air). For the competition studies, cells were incubated with 3 μmol/L [^{3}H]mitoxantrone or

[8] http://discover.nci.nih.gov/ and http://spheroid.ncifcrf.gov/spheroid/